TECHNICAL DEVELOPMENT REPORT NO. 392

THE CAA DOPPLER OMNIRANGE

FOR LIMITED DISTRIBUTION

by

Sterling R. Anderson
Robert B. Flint

Electronics Division

April 1959

FEDERAL AVIATION AGENCY
TECHNICAL DEVELOPMENT CENTER
INDIANAPOLIS, INDIANA

FEDERAL AVIATION AGENCY

E. R. Quesada, Administrator

D. M Stuart, Director, Technical Development Center

This is a technical information report and does not necessarily represent FAA policy in all respects

THE CAA DOPPLER OMNIRANGE

SUMMARY

This report describes a very high frequency omnirange (VOR), the operation of which is based upon an application of the Doppler effect Progress in the development of a Doppler VOR is outlined The Doppler VOR has a measured 7 to 1 improvement with respect to siting effects when compared to the conventional four-loop VOR The wave transmitted by the Doppler VOR is horizontally polarized The unique interchange in the functions of the 30-cps amplitude modulation and the 30-cps frequency modulation of a 9 96-kc subcarrier is described The Doppler VOR is shown to be compatible with the present VHF omnirange, and that its signals may be received on standard VOR receiving equipment

INTRODUCTION

Since 1952, the VHF omnirange (VOR) has been widely used as an air navigation aid and has become the International Civil Aviation Organization (ICAO) standard short-range air navigation system [1] The increasing use of the VOR in air traffic control operations places more stringent requirements on the location of omnirange stations Occasionally, a VOR location which is best suited for Federal Airways use geographically is in an environment where reflecting objects cause excessive course bends and scalloping Further, the environment of an established facility may change

The effects of various siting conditions on omnirange courses have been studied for the purpose of defining an offending object and establishing criteria for VOR site location [2] [3] The period and amplitude of course bends and scalloping are related to the distance between the ground station and the reflecting object, and to the projected area of the object normal to the arriving signal These relationships permit identification of the source of a reflection from a flight recording of the course information Because the effective azimuthal distribution of total VOR r-f energy is of necessity nondirectional, the solution to the reflection problem has been to remove the offending object or objects or to relocate the station These procedures are expensive and often impractical, and in some cases, are impossible

The recent development of the compatible Doppler VOR at the Technical Development Center (TDC) as opposed to a noncompatible Doppler omnirange previously reported by Hansel,[4] appears to be the most promising solution to VOR siting problems at difficult locations In August 1958, a prototype of the experimental Doppler VOR was installed and tested in a wooded area at Charleston, S C , where the conventional four-loop VOR already was installed Trees had been cleared to a radius of approximately 1,000 feet from the station, and the four-loop antenna system was mounted on a 75-foot high, 150-foot-diameter counterpoise The maximum scalloping error of the four-loop VOR was plus or minus 2 8° Under the same conditions, when the Doppler VOR was installed, maximum scalloping error was plus

[1] H C Hurley, S R Anderson, and H F Keary, "The CAA VHF Omnirange," Proceedings of the I R E , Vol 39 December 1951

[2] S R Anderson and H F Keary, "VHF Omnirange Wave Reflections from Wires," Technical Development Report No 126, May 1952

[3] Robert B Flint and Arthur E Frederick, "VHF Omnirange Reflections from a Single Tree," Technical Development Report No 314, June 1957

[4] Paul G Hansel, "Doppler-Effect Omnirange," Proceedings of the I R E , Vol 41, No 12, December 1953

or minus 0 4° Similar results were obtained during tests at the Technical Development Center at Indianapolis, Ind

This report presents a study of the Doppler VOR, the results of the development at Indianapolis, Ind , and the results of operational tests conducted at Charleston, S C

DESCRIPTION

The Doppler VOR, as the name implies, creates an effect in the received signal that is similar to the commonly observed Doppler effect normally associated with sound The cause of the Doppler effect in the received signal is the motion or position change of one of the two sources of radiation The motion of this source is accomplished by feeding successively each of 50 VHF loop antennas located on a circle 44 feet in diameter, thereby causing the point of the radiation source to rotate around this circle The virtual source is rotated at 30 revolutions per second (rps) A Doppler shift of plus or minus 480 cps created during each revolution, imposes a sinusoidal frequency modulation upon the signal at the receiver

A second source of radiation is obtained from a VHF loop antenna located in the center of the circle of 50 loops The r-f energy fed to the center antenna is amplitude modulated at 30 cps to produce the reference-phase, 30-cps signal in the receiver

Since the center antenna operates on the VOR channel frequency, while the 50 loops operate 9,960 cps above the VOR channel frequency, the plus or minus 480-cps Doppler shift also is imposed upon the 9,960-cps difference frequency [5] The phase of the 30-cps modulation of this frequency modulated difference frequency varies directly with the bearing of the receiver from the station The resulting 30-cps signal in the reference channel of the receiver therefore varies in phase with azimuth

Two transmitters are used to supply power to the antenna system The transmitter that supplies r-f energy to the center antenna is of high level, modulated with voice and identification signals The r-f output from this transmitter is mechanically modulated at 30 cps prior to being applied to the center antenna The output power of this transmitter is approximately ten times that of the transmitter output which is fed to the circle of 50 loops

The transmitter that supplies power to the circle of antennas is not modulated The distribution of the r-f energy for the 50 loops on the circle is accomplished through the use of a differential capacitor-distributor The action of the distributor, by feeding successively each loop on the circle, simulates one antenna on an arm 22 feet long rotating at 1,800 rpm

The radiation pattern of the center antenna is circular The radiation pattern of each antenna on the circle approaches an ellipse with some variation, depending upon the size of the counterpoise and the parasitic currents in adjacent antennas

Figure 1 is a view of the experimental Doppler omnirange at Indianapolis, Ind The counterpoise is 150 feet in diameter and 10 feet above ground level

THEORETICAL CONSIDERATIONS

In an attempt to explain briefly the operation of the CAA Doppler omnirange, an ideal antenna will be assumed, that is, an antenna that is located on the circumferenee of a circle and rotated around the center of the circle at a uniform velocity of 30 rps The aircraft is assumed to be motionless Figure 2 displays the situation in the horizontal plane, where

r = radius of the circle

ϕ = azimuthal angle of the aircraft

[5] The concept that the Doppler omnirange be made compatible with the conventional omnirange by providing a 9 96-kc difference frequency was first suggested to the authors by Mr. Henry C Hurley, Chief, Receiver Branch, Technical Development Center

R = distance from the center of antenna rotation to the aircraft

γ = azimuth angle of antenna

$\beta_2 = \frac{2\pi}{\lambda 2}$

λ_2 = wavelength

The wave traveling from the antenna to the aircraft undergoes an r-f phase delay

$$\psi = \beta_2 \left[R - r \cos(\phi - \gamma) \right] \tag{1}$$

The antenna is rotated in the counterclockwise direction at a uniform velocity pt, where t is time and $\frac{p}{2\pi}$ is a frequency. Hence

$$\gamma = pt \tag{2}$$

The signal at the aircraft then may be expressed as

$$E_2 = \cos \left[\omega_2 t + \beta_2 r \cos(\phi - pt) - \beta_2 R \right] \tag{3}$$

where

$\frac{\omega_2}{2\pi} = f_2$ = frequency of the current in the rotating antenna

$m_f = \frac{\text{variation of radio frequency away from the mean frequency}}{\text{modulation frequency}}$ = modulation index

as given by Terman [6]

Therefore,

$$m_f = \beta_2 r \tag{4}$$

The instantaneous frequency, f_{inst} of the wave represented by equation (3) is obtained by differentiation of the instantaneous angular velocity

$$f_{inst} = \frac{1}{2\pi} \frac{d}{dt} \left[\omega_2 t + \beta_2 r \cos(\phi - pt) - \beta_2 R \right]$$

$$f_{inst} = f_2 + \frac{rp}{\lambda} \sin(\phi - pt) \tag{5}$$

Up to this point it has been shown that by rotating an antenna, driven by r-f current of frequency f_2 at a uniform angular velocity about a vertical axis, a phase modulated wave is transmitted to the aircraft. The significant fact about this wave is that the phase of the modulation frequency is the azimuth angle of the aircraft ϕ. This is clearly shown in equation (3). It is interesting to observe that no error exists between the electrical phase angle and the azimuth of the aircraft. In order to extract this bearing intelligence, it is necessary to put the signal into a frequency discriminator in which the amplitude of the output voltage is a linear function of the instantaneous frequency of the input signal. Equation (5), containing the bearing information ϕ, expresses the instantaneous frequency of the signal impressed upon the discriminator input. The discriminator output, therefore, is a wave of frequency $\frac{p}{2\pi}$ which varies as the aircraft azimuth angle ϕ.

[6] F. E. Terman, Radio Engineers' Handbook, McGraw-Hill Book Co., Inc., 1943

Applying the constants of the CAA Doppler omnirange to the preceding equations results in the following

$r = 21\,796$ feet

$\frac{p}{2\pi} = 30$ cps

$118\,Mc > f_2 > 108\,Mc$

$m_f = \beta_2 r = \frac{2\pi}{8\,56} \times 21\,796 = 16$ for $f_2 = 115\,Mc$

$f_{inst}\,(cps) = 115 \times 10^6 + 480 \sin(\phi - pt)$

It should be noted that an FM wave, where $m_f = 16$ and the modulation frequency is 30 cps, is exactly compatible with the conventional VOR

An additional antenna is located at the center of rotation of the circle for the purpose of (1) conveying a reference 30-cps signal, and (2) providing a carrier 9 96-kc removed from the frequency modulated signal for converting the frequency of this signal to 9 96 kc at the output of the second detector of a conventional VOR receiver The signal received at the aircraft from the center antenna is

$$E_1 = \cos(\omega_1 t - \beta_1 R)(1 + m \cos pt) \tag{6}$$

where

$\frac{\omega_1}{2\pi} = f_1$ = frequency of the current in the center antenna

$\beta_1 = \frac{2\pi}{\lambda_1}$

λ_1 = wavelength

m = amplitude modulation index

Combining equations (3) and (6) represents an expression of the total signal at the aircraft

$$E = E_1 + nE_2 \tag{7}$$

where n is a constant regulating the relative amounts of the two signals

$$E = \left\{\cos(\omega_1 t - \beta_1 R)(1 + m \cos pt) + n \cos\left[\omega_2 t + \beta_2 r \cos(pt - \phi) - \beta_2 R\right]\right\} \tag{8}$$

The first term of equation (8) represents an amplitude modulated wave which conveys the reference or fixed-phase 30-cps portion of the signal, whereas the 30-cps variable phase signal is contained in the second term in the form of a frequency modulation

The CAA Doppler omnirange is compatible with the conventional omnirange and therefore the variables and constants of equation (8) are fixed at

$$\frac{\omega_2}{2\pi} - \frac{\omega_1}{2\pi} = \frac{\Delta}{2\pi} = 9\,96\ Kc \tag{9}$$

and

$m = n = 0\,3$

In Fig 3 is depicted the distribution of the signals radiated by the Doppler omnirange where the reference 30-cps signal is in the form of AM sidebands whereas the variable 30-cps signal is contained in the FM sidebands

Will the signal radiated by the CAA Doppler omnirange theoretically be exactly compatible with that of the conventional omnirange, and with a high degree of bearing accuracy? To answer this question the signal expressed by equation (8) is put into a linear detector and the output is analyzed This is ideally accomplished mathematically by analyzing the envelope of equation (8) [7] Combining equations (8) and (9) and assuming $\beta_2 R = \beta_1 R$

$$E = \sqrt{(1+m\cos a+n\cos b)^2+n^2\sin^2 b}\ \cos(\omega_1 t-\beta_1 R-\psi) \tag{10}$$

where

$a = pt$

$b = \Delta t+\beta_2 r\cos(pt-\phi)$

$$\psi = \tan^{-1}\left\{\frac{-n\sin\Delta t+\beta_2 r\cos(pt-\phi)}{1+m\cos pt+n\cos\left[\Delta t+\beta_2 r\cos pt-\phi\right]}\right\}$$

The output of the linear detector is proportional to

$$|E| = \sqrt{A^2+B^2} \tag{11}$$

where

$A = 1+m\cos a+n\cos b$

$B = n\sin b$

By means of the binomial expansion where $\left(\frac{B}{A}\right)^2 \leq 1$

$$|E| = A+\frac{B}{2}-\frac{1}{8}\frac{B^2}{A}+\frac{3}{48}\frac{B^3}{A^2}- \tag{12}$$

$$E = 1+m\cos a+n\cos b+\frac{1}{2}n\sin b-\frac{1}{8}\frac{n^2\sin^2 b}{1+m\cos a+n\cos b}+\frac{3}{48}\frac{n^3\sin^3 b}{(1+m\cos a+n\cos b)^2}- \tag{13}$$

The fifth term in equation (13) is expanded by means of the binomial theorem with the condition

$(m\cos a+n\cos b)^2 < 1$

$$\frac{1}{1+m\cos a+n\cos b} = 1-(m\cos a+n\cos b)+(m\cos a+n\cos b)^2-(m\cos a+n\cos b)^3+ \tag{14}$$

By substituting equation (14) in equation (13) and retaining only the first five terms of equation (13)

$$|E| = 1+m\cos a+n\frac{\sqrt{5}}{2}\cos(b-\tan^{-1}\tfrac{1}{2})-\frac{n^2}{8}\left[\sin^2 b-\sin^2 b(m\cos a+n\cos b)+\sin^2 b(m\cos a+n\cos b)^2-\ \right] \tag{15}$$

Finally, by combining terms of the same frequency in equation (15), letting m = n = 0 3, and neglecting the d-c components the output of the linear detector becomes

$$\begin{aligned}|E| = {} & 0\,3017\cos pt+0\,337\cos\left[\Delta t+\beta_2 r\cos(pt-\phi)-26\,5^\circ\right] \\ & -000169\cos pt\cos\left[2\Delta t+2\beta_2 r\cos(pt-\phi)\right] \\ & -000084\cos\left[3\Delta t+3\beta_2 r\cos(pt-\phi)\right] \\ & +\end{aligned} \tag{16}$$

[7] C B Aiken, "Theory of the Detection of Two Modulated Waves by a Linear Rectifier," Proceedings of the I R E , pp 601-629, April 1933

Equation (16) indicates clearly that the ideal linear detector will transform the signal from the CAA Doppler omnirange into a distortionless reference 30-cps signal, and a distortionless 9 96-kc subcarrier signal which is frequency modulated with a 30-cps variable phase signal The phase of the variable phase signal is the azimuth angle Therefore, the bearing accuracy is expected to be excellent The third and fourth terms of equation (16) represent frequencies of 2 x 9 96 kc and 3 x 9 96 kc, respectively, and would be expected to have negligible effect on the omnirange receiver performance The terms neglected in the series of equation (16) are expected to be smaller than any term included, and also of higher frequency

It is demonstrated that a Doppler omnirange compatible with the conventional VHF omnirange is feasible It generally is found in the field of navigational aids for aircraft that siting error in the bearing caused by reflections of r-f energy from objects near the transmitter is inversely proportional to some function of the size of the antenna system It is desired to show theoretically the amount and nature of the improvement in siting errors that might be expected from the CAA Doppler omnirange compared with the conventional omnirange

Figure 4 depicts the situation to be studied where one reflecting object is located d_1 distance east of the transmitting antenna of the Doppler omnirange or the conventional omnirange An aircraft is located at ρ, at azimuth angle ϕ The reflecting object radiates a circular pattern The signals arriving at the aircraft follow two paths, i e , along r_0 and r_1 The signal traveling along r_0 contains the correct bearing information ϕ, whereas the reflected signal contains bearing information of $\phi = 90°$ The symbols in the following equations have the same meaning as the corresponding equations given previously The signal[8] at point p is derived as follows

The direct wave is given by

$$E(\phi) = \frac{\cos(\omega_1 t - \beta_1 r_0)}{r_0}(1 + m \cos pt) + \frac{n}{r_0}\cos[\omega_2 t + \beta_2 r \cos(pt - \phi) - \beta_2 r_0] \qquad (17)$$

The reflected wave is given by

$$E(90°) = \frac{A \cos(\omega_1 t - \beta_1 r_1 - \delta)}{r_1}(1 + m \cos pt) + \frac{An}{r_1}\cos(\omega_2 t + \beta_2 r \sin pt - \beta_2 r_1 - \delta) \qquad (18)$$

where

δ = r-f phase change caused by the reflector

r = radius of circle of Doppler omnirange antenna system

r_0 = direct path

r_1 = indirect path via reflecting object

A = ratio of amplitude of the reflected signal divided by amplitude of the direct signal appearing at aircraft

Since $\frac{1}{r_0} \approx \frac{1}{r_1}$, the total signal at the aircraft becomes

[8]The mathematical analysis is similar to one appearing in "Frequency Modulation Propagation Characteristics," by Murray G Crosby, Proceedings of the Institute of Radio Engineers Volume 24, No 6, June 1936 It was suggested to the authors in an unpublished memorandum by Fred Moskowitz of Rome Air Development Center, Griffiss AFB, Rome, N Y

$$E(\phi)+E(90^\circ)=\frac{1}{r_0}\left\{\left[\cos(\omega_1 t-\beta_1 r_0)+A\cos(\omega_1 t-\beta_1 r_1-\delta)\right]\right.$$
$$(1+m\cos pt)+n\cos\left[\omega_2 t+\beta_2 r\cos(pt-\phi)-\beta_2 r_0\right]$$
$$\left.+An\cos(\omega_2 t+\beta_2 r\sin pt-\beta_2 r_1-\delta)\right\} \qquad (19)$$

The last two terms in equation (19) represent the desired phase modulation signal which conveys the azimuthal intelligence and the reflected phase modulation signal, respectively In order to determine the bearing error incurred because of a reflection from an object at 90° azimuth, the last two terms of equation (19) are combined It is only the instantaneous phase angle of the resultant signal that is required for a determination of bearing error

Then

$$\phi_P=\beta_2 r\cos(pt-\phi)-\beta_2 r_0+A\sin\left[\beta_2 r\sin pt\right.$$
$$\left.-\beta_2 r_1-\delta-\beta_2 r\cos(pt-\phi)+\beta_2 r_0\right] \qquad (20)$$

where

$\phi_P \approx$ instantaneous phase of the resultant signal

$A \leq 0\ 1$

and

$$\phi_P=\beta_2 r\cos(pt-\phi)-\beta_2 r_0+A\sin\left[2\beta_2 r\sin\left(\frac{90^\circ-\phi}{2}\right)\right.$$
$$\left.\sin\left(pt-\frac{90^\circ+\phi}{2}\right)+\beta_2(r_0-r_1)-\delta\right] \qquad (21)$$

or

$$\phi_P=\beta_2 r\cos(pt-\phi)-\beta_2 r_0$$
$$+2A\cos\left[\beta_2(r_0-r_1)-\delta\right]\sum_{n=0}^{\infty} J_{2n+1}\left(2\beta_2 r\sin\left(\frac{90^\circ-\phi}{2}\right)\right)\sin\left[(2n+1)\left(pt-\frac{90^\circ+\phi}{2}\right)\right]$$
$$+A\sin\left[\beta_2(r_0-r_1)-\delta\right]J_0\left(2\beta_2 r\sin\left(\frac{90^\circ-\phi}{2}\right)\right)$$
$$+2A\sin\left[\beta_2(r_0-r_1)-\delta\right]\sum_{n=1}^{\infty} J_{2n}\left(2\beta_2 r\sin\left(\frac{90^\circ-\phi}{2}\right)\right)\cos\left[2n\left(pt-\frac{90^\circ+\phi}{2}\right)\right] \qquad (22)$$

where

$J_0(\ \ )$, $J_{2n+1}(\ \ )$, $J_{2n}(\ \ )$ are Bessel functions of the first kind

The output of an ideal discriminator is proportional to the instantaneous frequency of the input signal The instantaneous frequency is equal to $\frac{1}{2\pi}\frac{d\phi_p}{dt}$

Therefore

$K\frac{d\phi p}{dt} = \imath_P$ = discriminator output current

where

K = a constant of proportionality

$$\theta_p = -\beta_2 r\, p \sin(pt-\phi) + 2Ap\cos\left[\beta_2(r_0-r_1)-\delta\right] J_1\left(2\beta_2 r \sin\left(\frac{90^\circ-\phi}{2}\right)\right)\cos\left(pt-\frac{90^\circ+\phi}{2}\right)$$

$$-4Ap\sin\left[\beta_2(r_0-r_1)-\delta\right] J_2\left(2\beta_2 r \sin\left(\frac{90^\circ-\phi}{2}\right)\right)\sin(2pt-90^\circ-\phi)$$

$$+6Ap\cos\left[\beta_2(r_0-r_1)-\delta\right] J_3\left(2\beta_2 r \sin\left(\frac{90^\circ-\phi}{2}\right)\right)\cos\left(3pt-\frac{270^\circ-3\phi}{2}\right)+ \qquad (23)$$

At the discriminator output of the conventional omnirange receiver, there are filters that favor the fundamental frequency $\frac{P}{2\pi}$, and tend to reject the harmonics of $\frac{P}{2\pi}$. Assuming that only the fundamental frequency terms of equation (23) are effective in the receiving equipment for determining the bearing, the infinite number of terms after the first two are neglected. Combining the first two terms of equation (23)

$$\theta_p = \pm\sqrt{(\beta_2 rp)^2 + (2Ap)^2\cos^2\left[\beta_2(r_0-r_1)-\delta\right] J_1^2\left(2\beta_2 r \sin\left(\frac{90^\circ-\phi}{2}\right)\right)}$$

$$+4\beta_2 rp^2 A\cos\left[\beta_2(r_0-r_1)-\delta\right] J_1\left(2\beta_2 r \sin\left(\frac{90^\circ-\phi}{2}\right)\right)\sin\left(\frac{\phi-90^\circ}{2}\right)$$

$$\sin\left\{pt-\phi+\tan^{-1}\left[\frac{2A\cos\left[\beta_2(r_0-r_1)-\delta\right] J_1\left(2\beta_2 r \sin\left(\frac{90^\circ-\phi}{2}\right)\right)\cos\left(\frac{\phi-90^\circ}{2}\right)}{\beta_2 r + 2A\cos\left[\beta_2(r_0-r_1)-\delta\right] J_1\left(2\beta_2 r \sin\left(\frac{90^\circ-\phi}{2}\right)\right)\sin\left(\frac{\phi-90^\circ}{2}\right)}\right]\right\} \qquad (24)$$

Finally, the resultant $\frac{P}{2\pi}$ phase angle is obtained as shown in equation (24). The error caused by the reflected wave is the $\tan^{-1}[\quad]$ term. In equation (24) it can be seen that, if no reflection occurs, A = 0.

Then

$$\theta_p = -\beta_2 rp \sin(pt-\phi) \qquad (25)$$

The error, designated by x, caused by the reflecting object located at 90° azimuth, becomes

$$x \approx \frac{2AJ_1\left(2\beta_2 r \sin\left(\frac{90^\circ-\phi}{2}\right)\right)\cos\left(\frac{\phi-90^\circ}{2}\right)\cos\left[\beta_2(r_0-r_1)-\delta\right]}{\beta_2 r} \qquad (26)$$

since

$A \leq 0.1$

It is clear from equation (26) that x, the bearing error, varies as the aircraft moves, because $(r_0 - r_1)$ is a function of the aircraft position.[9] Hence this error oscillates as $\cos[\beta_2 (r_0 - r_1) - \delta]$ varies from plus 1 to 0 then to minus 1 and so forth. This is called scalloping of the bearing indication. The maximum values of equation (26) are plotted in Fig. 5, when A = 0.10. For comparison the scalloping associated with a conventional omnirange[10] is plotted in Fig. 6, where the scalloping of the Doppler omnirange is plotted to the same scale. A comparison of the scalloping of the two omnirange systems is shown in Fig. 7. It is interesting to note that the scalloping of the Doppler omnirange as shown in Fig. 7 has a reduction factor of 0.1 or less for most azimuths. This means that the scalloping associated

[9] This is treated in some detail in "VHF Omnirange Wave Reflections from Wires," by S. R. Anderson and H. F. Keary, Technical Development Report No. 126, Technical Development Center, May 1952.

[10] Sterling R. Anderson, Robert B. Flint, William L. Wright, and John Turk, Preliminary Tests of a Precision VHF Omnirange," Technical Development Report No. 355, August 1958.

with a conventional omnirange will be reduced by a factor of 10 at most azimuths by replacing the conventional omnirange with a Doppler omnirange Figure 7 also indicates that there is a sector of approximately 10°, centered on $\phi = 90°$, where little reduction in scalloping will be obtained by replacing a conventional omnirange with a Doppler omnirange This phenomenon is borne out qualitatively in practice where the reflecting source consists of two vertical towers approximately 60 feet high located 880 feet distant at 266° azimuth and 285° azimuth, respectively, from the omnirange These towers are the two located immediately behind the Doppler omnirange shown in Fig 1 The sinusoidal scalloping in Fig 18 in the vicinity of 250° azimuth and 270° azimuth is caused by these two towers

EQUIPMENT

A block diagram of the Doppler omnirange is shown in Fig 8 The antenna system uses 51 VHF loop antennas designed to operate in the 108- to 118-Mc range They are supported on pedestals at approximately one-half wavelength above a wire screen counterpoise Type RG 8/U transmission line is used throughout Figure 9 is a view of the Doppler VOR antenna system

The transmitter and modulation equipment used to supply r-f power to the center antenna are of conventional design This transmitter is capable of supplying 200 watts r-f power continuously Plate modulation is employed to provide the station with voice intelligence and a keyed 1020-cps identification signal

The 30-cps modulation of the transmitter output is accomplished by means of a capacity goniometer and a transmission line VHF bridge network Referring to Fig 8, it will be noted that the transmitter output is fed directly to a power divider which is followed by a modulation eliminator The purpose of the modulation eliminator is the same as that in the conventional VOR system [11] The smaller amount of the r-f power divider apportionment, having the modulation removed, is fed to the input of a capacity goniometer The capacity goniometer is a conventional type used in the standard VOR One output of the goniometer is fed to a Termaline dummy load The other output, consisting only of 30-cps sideband energy, is fed to an input corner of the VHF bridge network This sideband energy is combined with the carrier energy at the output corner of the bridge thereby amplitude-modulating the carrier to approximately 30 per cent The r-f power at the output corner of the bridge is fed through coaxial transmission line to the center antenna

Present plans include the possible use of a 30-cps alternator to modulate the carrier This would preclude the necessity of the bridge network, goniometer, and the modulation eliminator used to provide 30-cps modulation of the carrier

A separate transmitter is used to supply r-f power to the circle of 50 antennas This transmitter is crystal-controlled at a frequency 9,960 cps higher than the frequency of the carrier The differential capacitor distributor feeds each antenna in succession The r-f power applied to the input of the distributor is fed through a rotating element of a capacitor in the form of concentric cylinders, thence through coaxial line in a bore along the motor shaft to a single plate located on the periphery of a disc of insulating material The disc, which is approximately 9 inches in diameter is attached to the shaft of the synchronous motor and rotates at 1,800 rpm Fifty stationary plates encompass the arc of the rotor plate

The disassembled distributor is shown in Fig 10 Note that alternate stator plates are displaced vertically This is done to minimize coupling between adjacent plates The r-f energy is capacitively coupled to each stator plate in succession as the rotor revolves The distributor output terminations are connected directly to the stator plates The voltage wave-shape at the output terminations is sinusoidal Ideally, any one output is zero during 345 6° of each rotation of the rotor During the remaining 14 4°, the output voltage rises to a maximum and falls back to zero The sinusoids are spaced equally on a circle with adjacent spacing (maximum to maximum) of 7 2° Expressed mathematically

[11] H C Hurley, S R Anderson and H F Keary, "The CAA VHF Omnirange," Technical Development Report No 113, June 1950

$E_1 = \sin 12\,5\theta$ $\quad 0° \leq \theta \leq 14\,4°$

$E_2 = \sin (12\,5\theta - 90°)$ $\quad 7\,2° \leq \theta \leq 21\,6°$

$E_3 = \sin (12\,5\theta - 180°)$ $\quad 14\,4° \leq \theta \leq 28\,8°$

$E_n = \sin [12\,5\theta - 90°(n-1)]$ $\quad 7\,2(n-1) \leq \theta \leq 14\,4° + 7\,2°(n-1)$

$E_{50} = \sin(12\,5\theta - 4410°)$ $\quad 352\,8° \leq \theta \leq 367\,2°$

where

θ = the angle of rotation of the rotor

E_1 = voltage of No 1 output

E_n = voltage of No n output

n = the output number

To minimize transients, a 100-ohm nonreactive resistor was connected in parallel with each transmission line at the output terminations of the distributor Figure 11 shows the distributor unit in normal operation with all lines connected

Although the present system utilizing a separate transmitter for the circle of 50 antennas has proved to be successful and sufficiently stable with respect to the 9960-cps difference frequency, a modification is contemplated that probably will replace this transmitter with a frequency converter unit The frequency converter unit will be excited and controlled by the transmitter used in conjunction with the center antenna Also, the distributor unit will be connected mechanically to the synchronous motor and reference 30-cps alternator or goniometer This will prevent any possibility of an erroneous phase relationship between the two 30-cps signals in the VOR receiver

TESTS

During the development of the CAA Doppler omnirange a counterpoise 75 feet in diameter and 10 feet high was used to support 50 loop antennas mounted 48 inches above the counterpoise and equally spaced around a 22-foot radius circle The 22-foot radius circle is concentric with the counterpoise

A special test was conducted in which the 50 loops were removed from atop the counterpoise and a single loop was placed on the circle Field strength measurements were made at a distance of 1/2-mile with the single loop fed directly from the transmitter The single loop was moved to every even-numbered mounting position for each measurement of field strength The data, plotted in Fig 12, show a variation in field strength of plus or minus 22 6 per cent about a mean value due to the counterpoise eccentricity effect

A reduction of the counterpoise eccentricity effect was obtained by extending the diameter of the counterpoise from 75 feet to 150 feet The field strength measurements were repeated and these data are plotted in Fig 13 The field strength variation shown in Fig 13 caused by counterpoise eccentricity effect, is 9 82 per cent This is a marked improvement over the 75-foot diameter counterpoise However, there is considerable modification of these patterns when the distributor and 50 loops are used The r-f coupling between any driven stator plate and an adjacent stator plate in the engineering model distributor, and mutual couplings between antennas, cause a different pattern to be radiated in operation The envelope of the 9960-cps signal is proportional to the amplitude of the field strength radiated by the 50 loops An oscillogram of the 9960-cps signal in a receiver located 200 feet distant is shown in Fig 14 The large variations in amplitude of the 9960-cps signal, which occur at a 30-cps rate, cause a cross modulation of the 30-cps signal in the AM channel of the receiver The cross modulation causes a bearing error which varies with azimuth, as evidenced by the shape of the Doppler bearing error curve, Fig 16 The resulting maximum bearing error is approximately plus or minus 1°

The small sinusoidal changes in amplitude in Fig 14 occur at a 1500-cps rate These are due to the variation in field strength caused by a transition from one pattern when a single antenna is being fed to another pattern when two antennas are being fed This amplitude modulation of the subcarrier causes a 1500-cps signal in the audio output of the receiver, but only in strong signal areas Such areas are encountered when the aircraft is at an altitude of 2,000 feet and less than 5 miles from the ground station The 1500-cps signal has no effect on the course deviation indicator (CDI)

Figure 15 shows the antenna current distribution when the rotor was stopped at one stator The field pattern associated with these currents and the counterpoise eccentricity effect determine the field pattern radiated by the 50 loops

The bearing error data obtained from orbital flights at an approximately 6-mile radius are shown in Fig 16 The bearing error curve of a conventional VOR at the same site also is shown in Fig 16 in order that a comparison may be made between the two VOR systems

Radial flights were made while recording various signals in the receiver The recordings are reproduced in Fig 17 The reference channel 30-cps signal, which is the variable phase signal in the Doppler omnirange system, decreases in amplitude with an increase in elevation angle This would be expected theoretically because the motion toward or away from the observer of the virtual source appears to decrease with an increase of elevation angle This decrease has a 'softening' effect on the CDI TO-FROM and flag indicators While passing through the cone over the station, there is a short period of time when the flag alarm shows and the 1500-cps background level increases sharply in the audio channel

Figure 18 is a reproduction of flight recordings of the conventional VOR and the Doppler VOR located at the TDC test site The course roughness and scalloping caused by trees and buildings noted on the conventional VOR recording are essentially eliminated in the recording of the Doppler VOR The remaining scalloping in the 250° and 270° sectors is caused by two steel towers 60 feet high located west of the VOR site at a distance of 880 feet These may be seen in the foreground in Fig 1 Polarization error has been measured during flight tests on several Doppler omnirange stations and found to be less than plus or minus 1/2°

TESTS AT CHARLESTON, S C

The tests at the relatively good site at the Technical Development Center at Indianapolis indicated so much reduction of siting error that further tests were conducted at Charleston, S C where a 150-foot diameter counterpoise, 75 feet above the ground, was installed The site has trees beyond 2,000 feet from the tower in all directions for miles Previous tests with a conventional four-loop VOR antenna on the tower showed a maximum scalloping of plus or minus 2 8° during a 20-mile orbital flight The flight data on the Doppler VOR showed a maximum scalloping of plus or minus 0 4° Figure 19 is a reproduction of the flight recordings made at the Charleston site of the conventional omnirange and the Doppler omnirange

CONCLUSIONS

It is concluded that the principle of movement of a source of electromagnetic radiation can be used to provide azimuth information for aircraft Furthermore, it has been demonstrated that there is a distinct advantage in the Doppler principle over the pattern directivity principle of the conventional omnirange Specifically, the Doppler principle has the characteristic that the antenna aperture does not introduce ambiguities into the bearing data On the other hand, the conventional omnirange can be made to have a large aperture, but only by introducing ambiguities into the bearing information

The following results were obtained in the development of the CAA Doppler omnirange

1 The Doppler omnirange principle, when applied to an antenna array with an aperture of approximately 5 wavelengths and consisting of 50 loop antennas fed by a capacity type distributor, is feasible

2 The Doppler omnirange markedly reduces the siting error compared with the conventional omnirange

3 The Doppler omnirange is compatible with the conventional omnirange

4 The maximum bearing errors of the two omnirange systems are comparable and are approximately equal to plus or minus 1 0°

5 The cone characteristics of the Doppler omnirange are satisfactory Reduced course sensitivity was measured over the station

6 The Doppler omnirange polarization error is small compared to the conventional omnirange polarization error

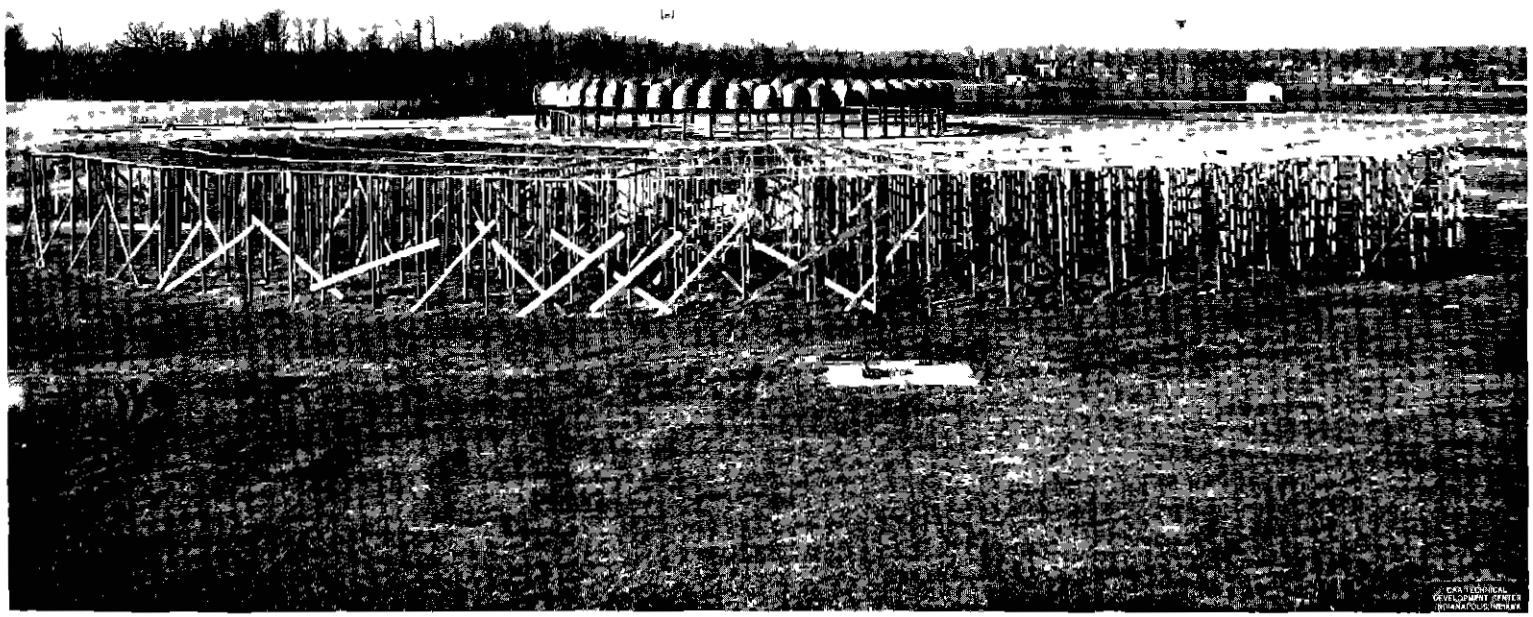

FIG. 1 THE EXPERIMENTAL DOPPLER OMNIRANGE AT INDIANAPOLIS, IND.

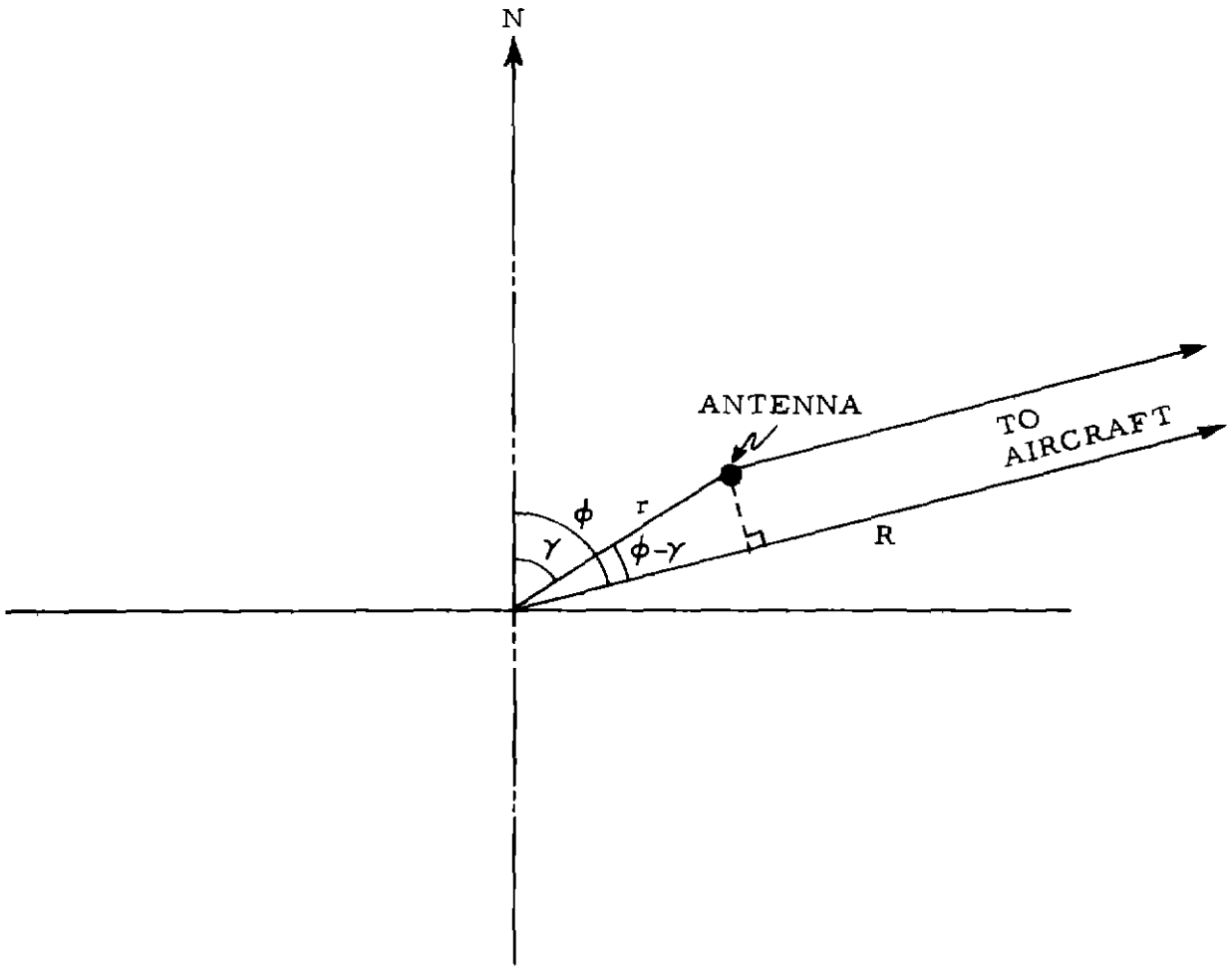

FIG. 2 THE COORDINATE SYSTEM FOR ONE TRANSMITTING ANTENNA

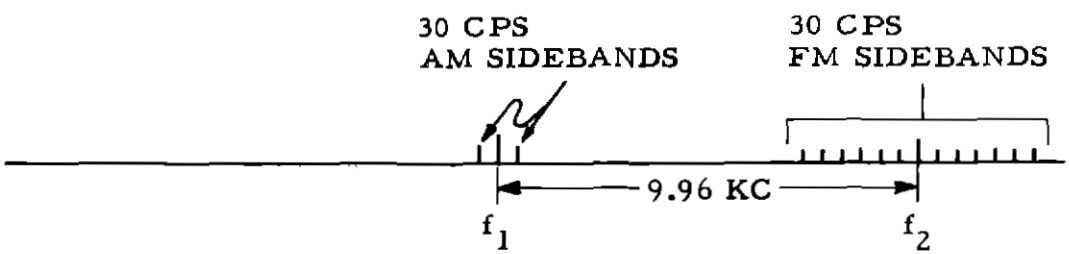

$108\ MC \leq f_1 \leq 118\ MC$

$f_2 > f_1$

FIG. 3 FREQUENCY SPECTRUM SHOWING SIDEBANDS AND CARRIER

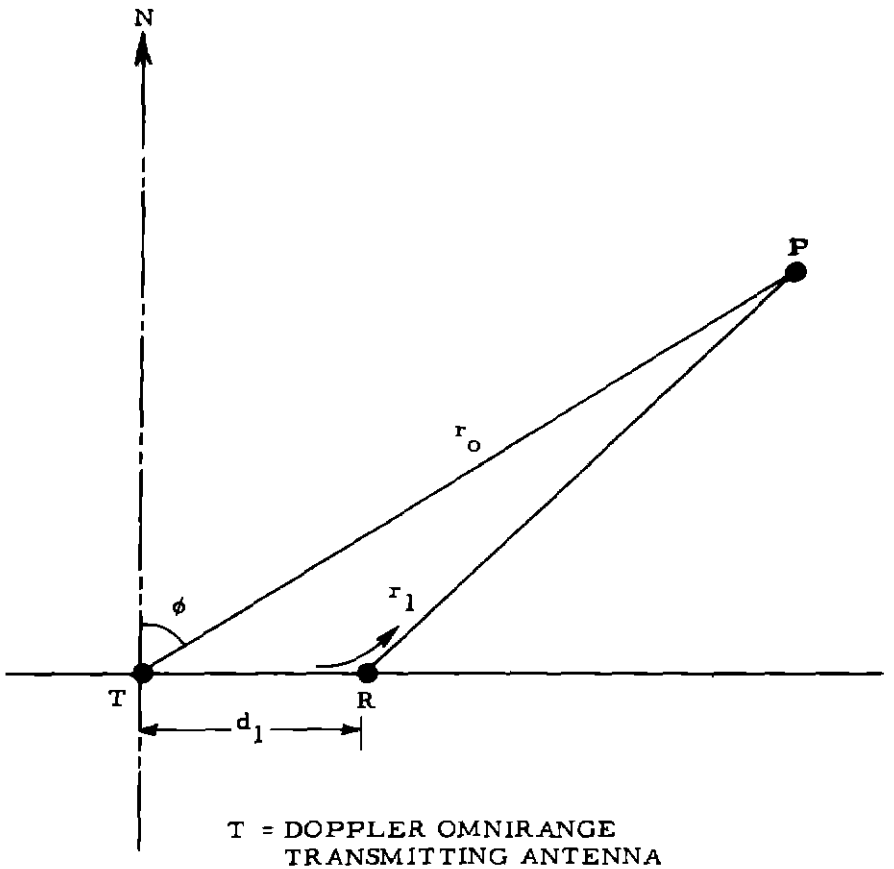

FIG. 4 A PLAN VIEW OF THE DOPPLER OMNIRANGE AND ONE REFLECTING OBJECT

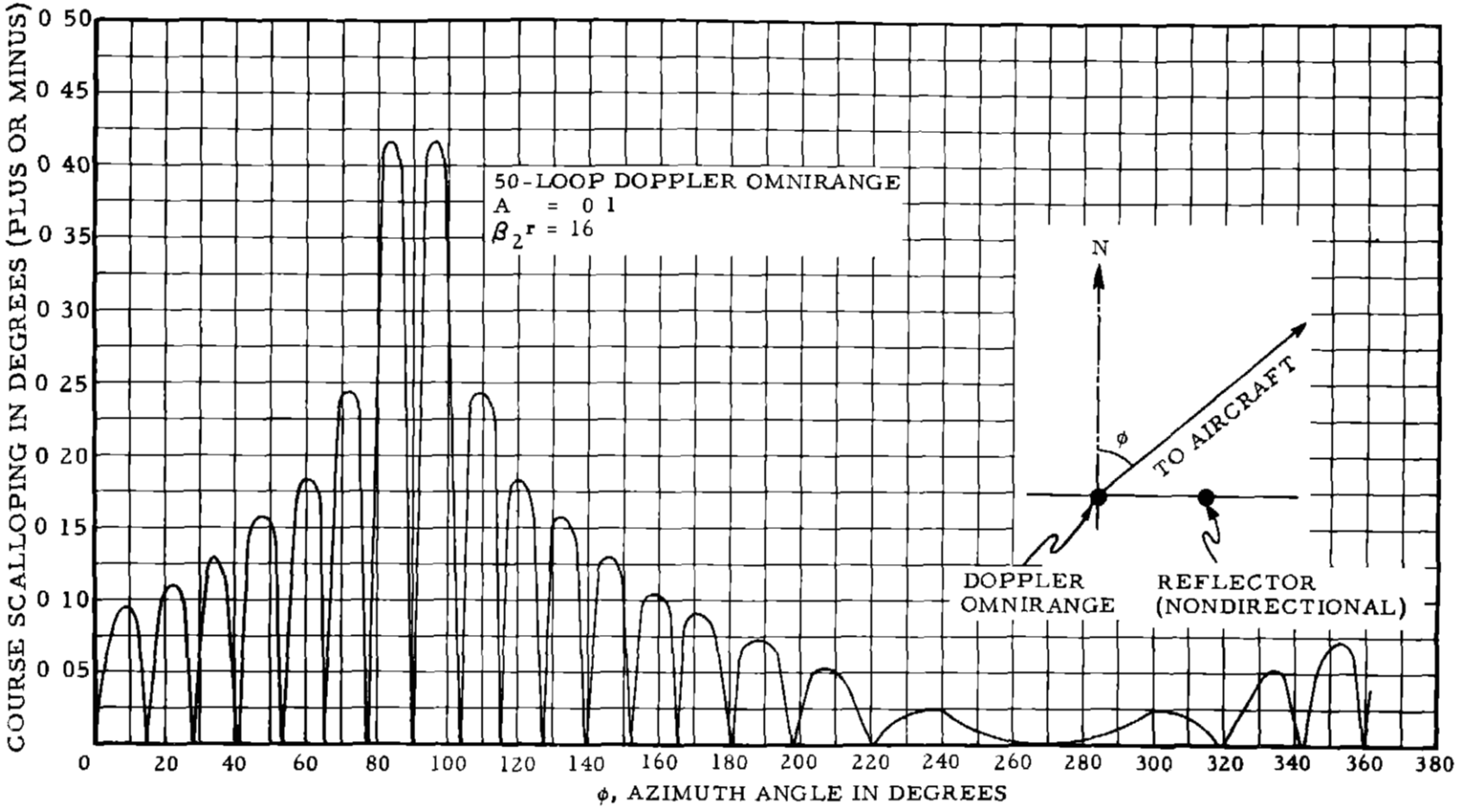

FIG. 5 THE THEORETICAL DOPPLER OMNIRANGE COURSE SCALLOPING CAUSED BY ONE REFLECTING OBJECT VERSUS AZIMUTH ANGLE

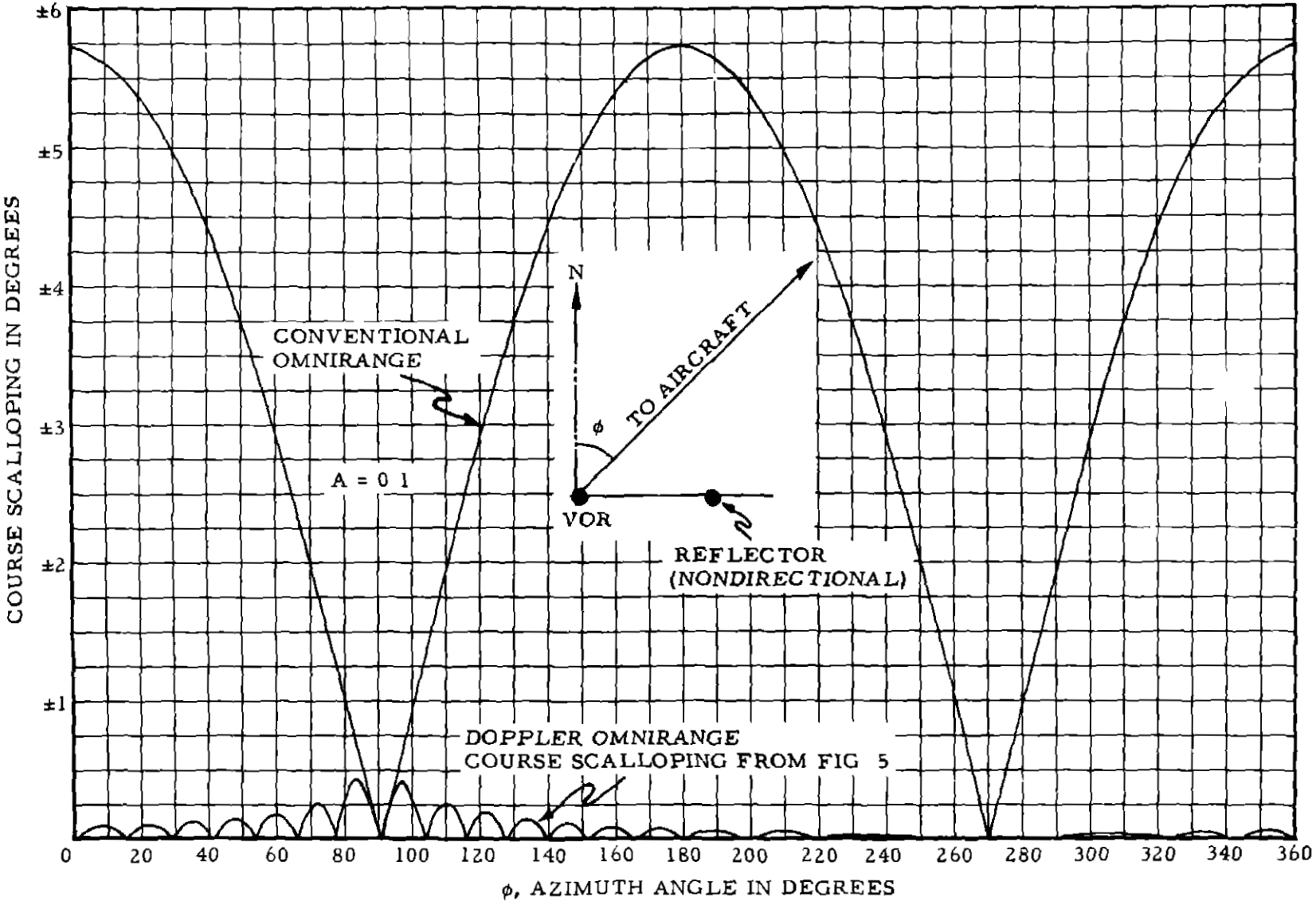

FIG 6 THEORETICAL COURSE SCALLOPING CAUSED BY ONE REFLECTING OBJECT *VERSUS AZIMUTH ANGLE*

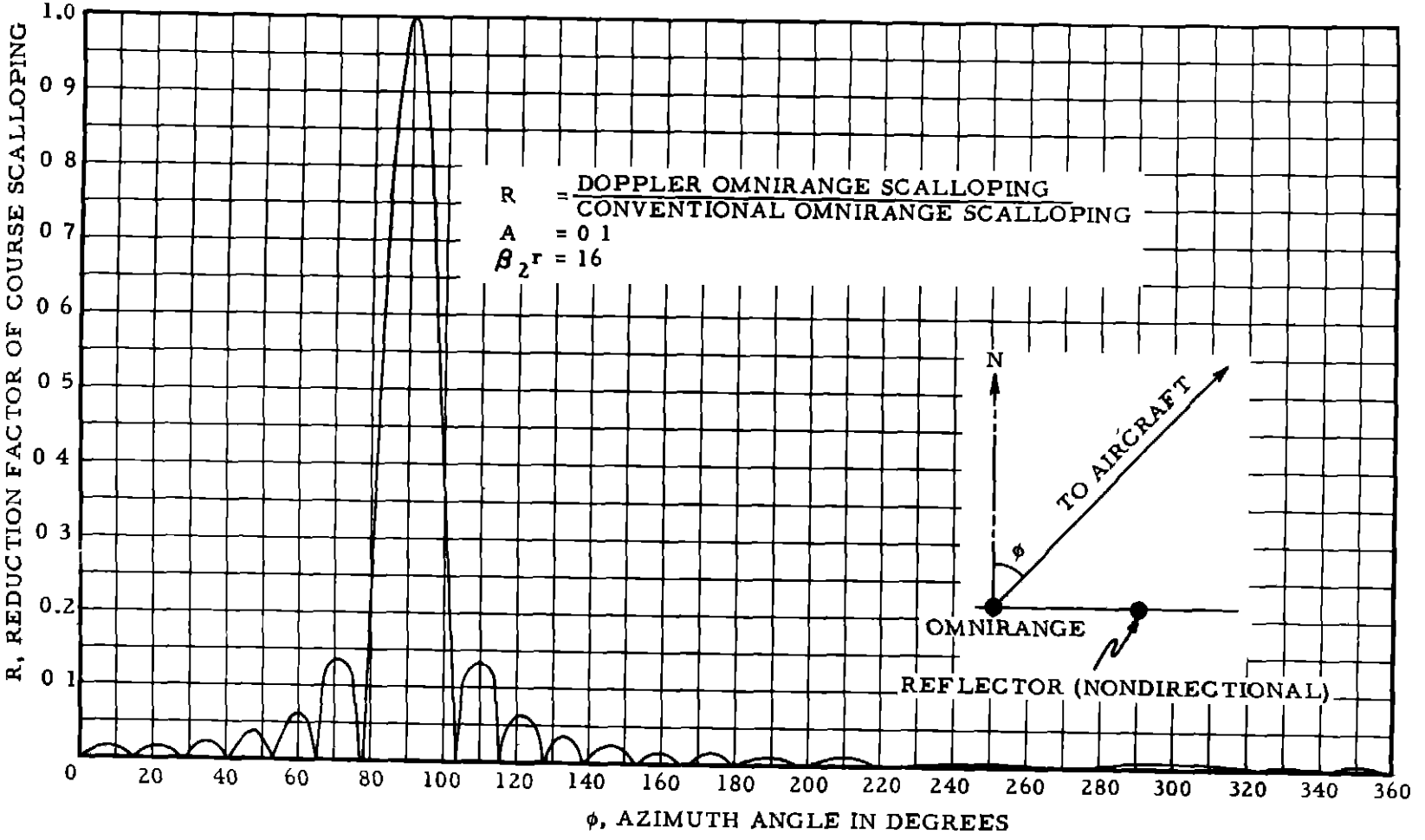

FIG 7 THEORETICAL REDUCTION IN VOR COURSE SCALLOPING EFFECTED BY THE DOPPLER OMNIRANGE

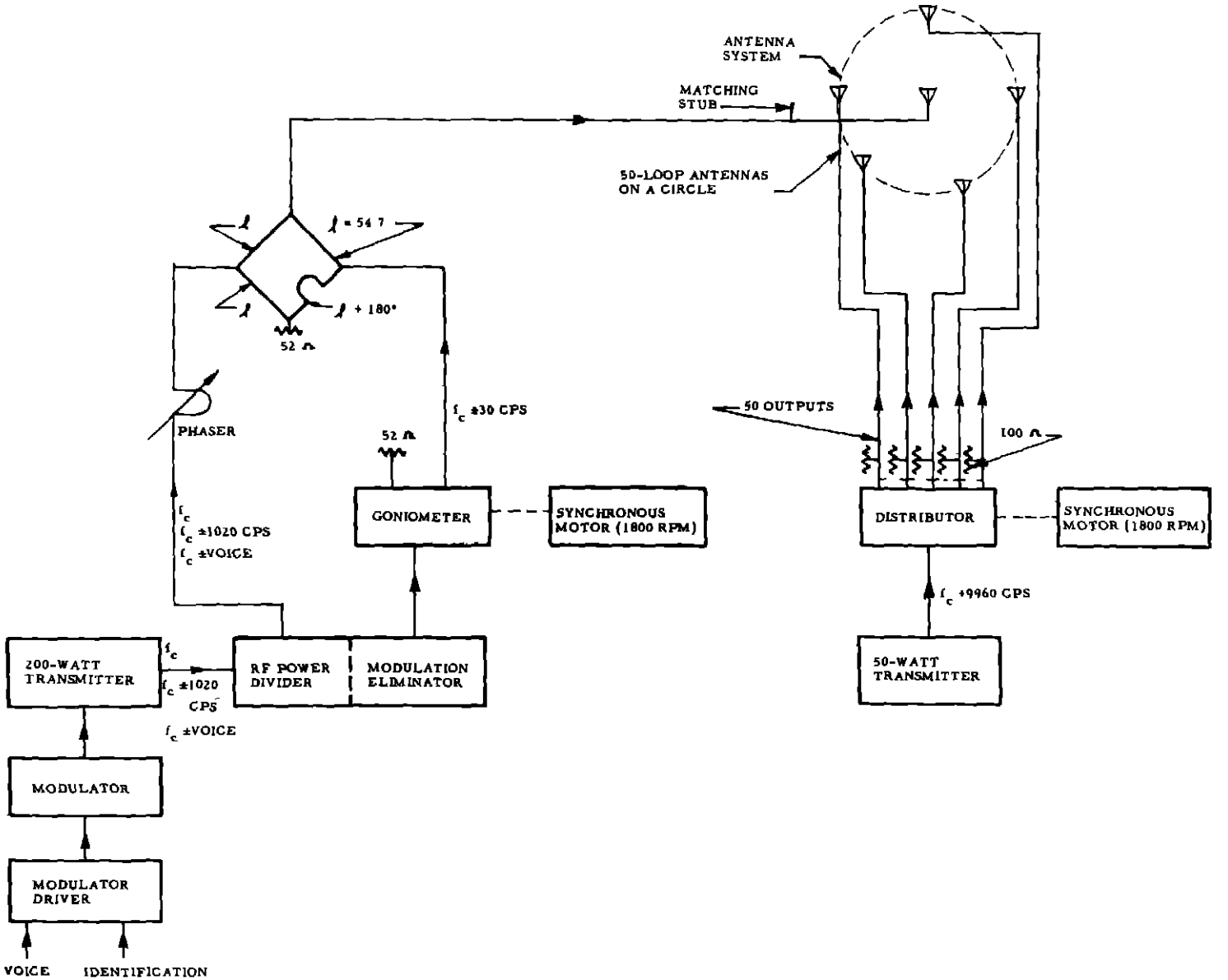

FIG 8 BLOCK DIAGRAM OF DOPPLER OMNIRANGE EQUIPMENT

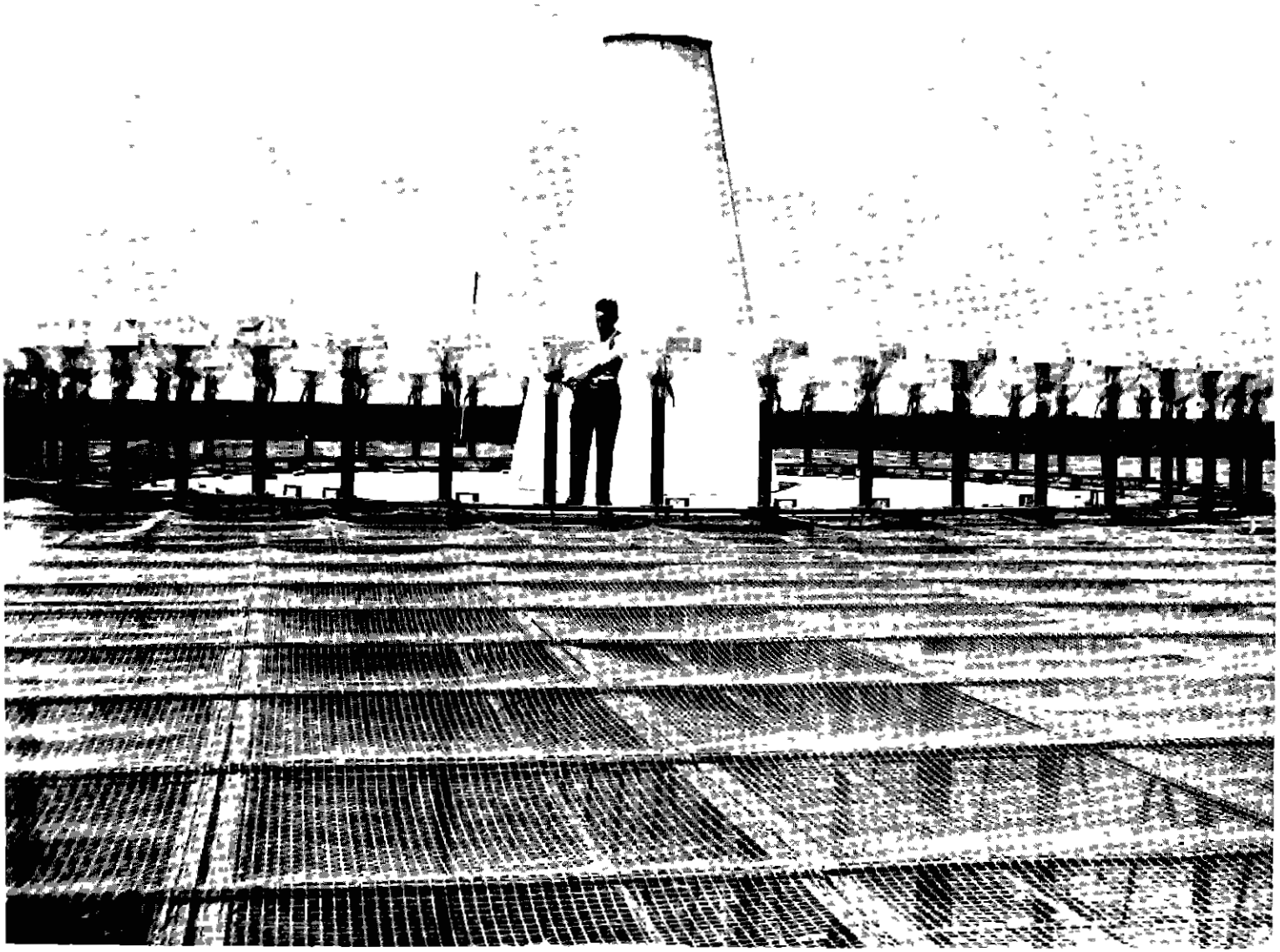

FIG. 9 THE DOPPLER VOR ANTENNA SYSTEM

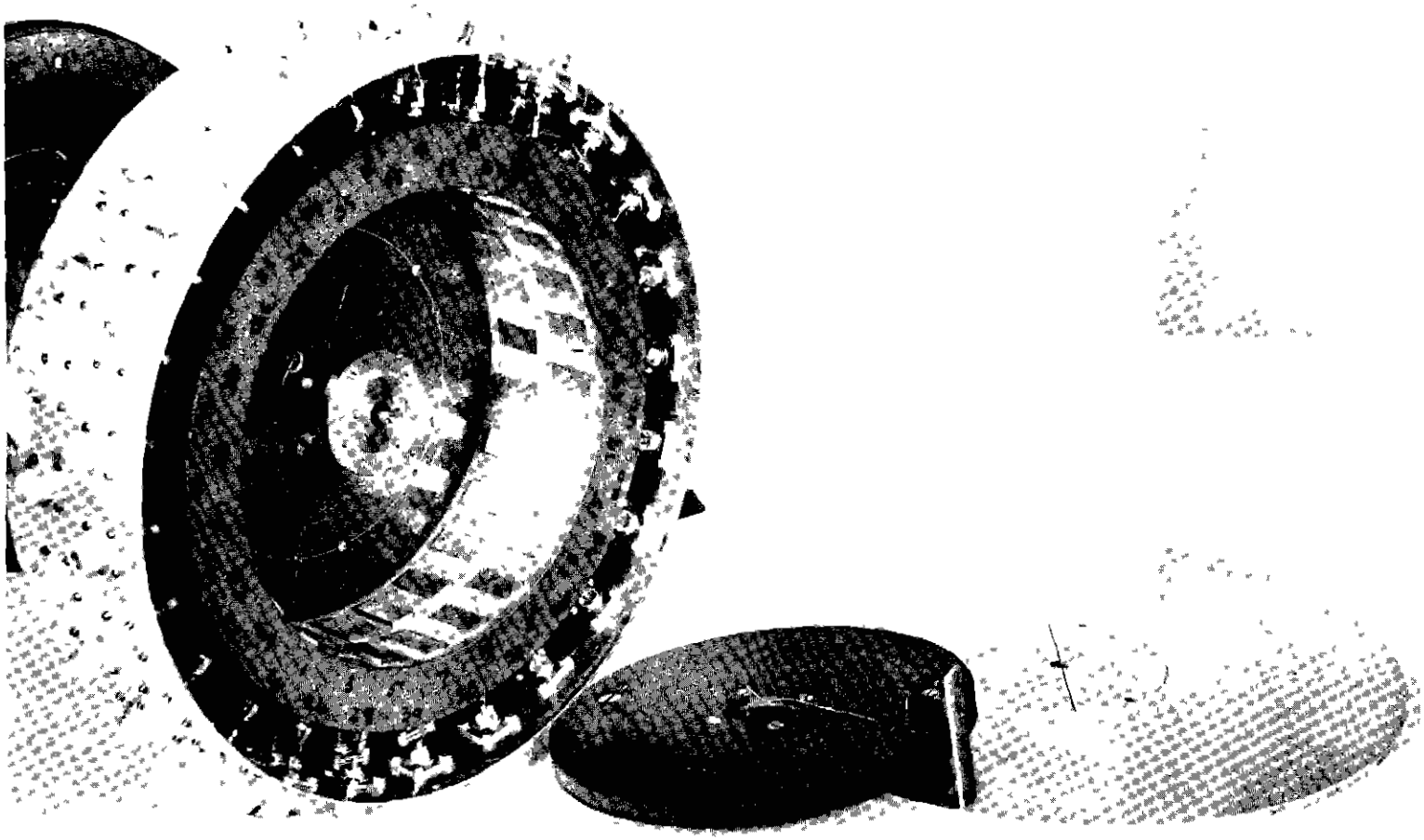

(A) DISTRIBUTOR HEAD

FIG 10 THE DOPPLER VOR DIFFERENTIAL CAPACITOR DISTRIBUTOR

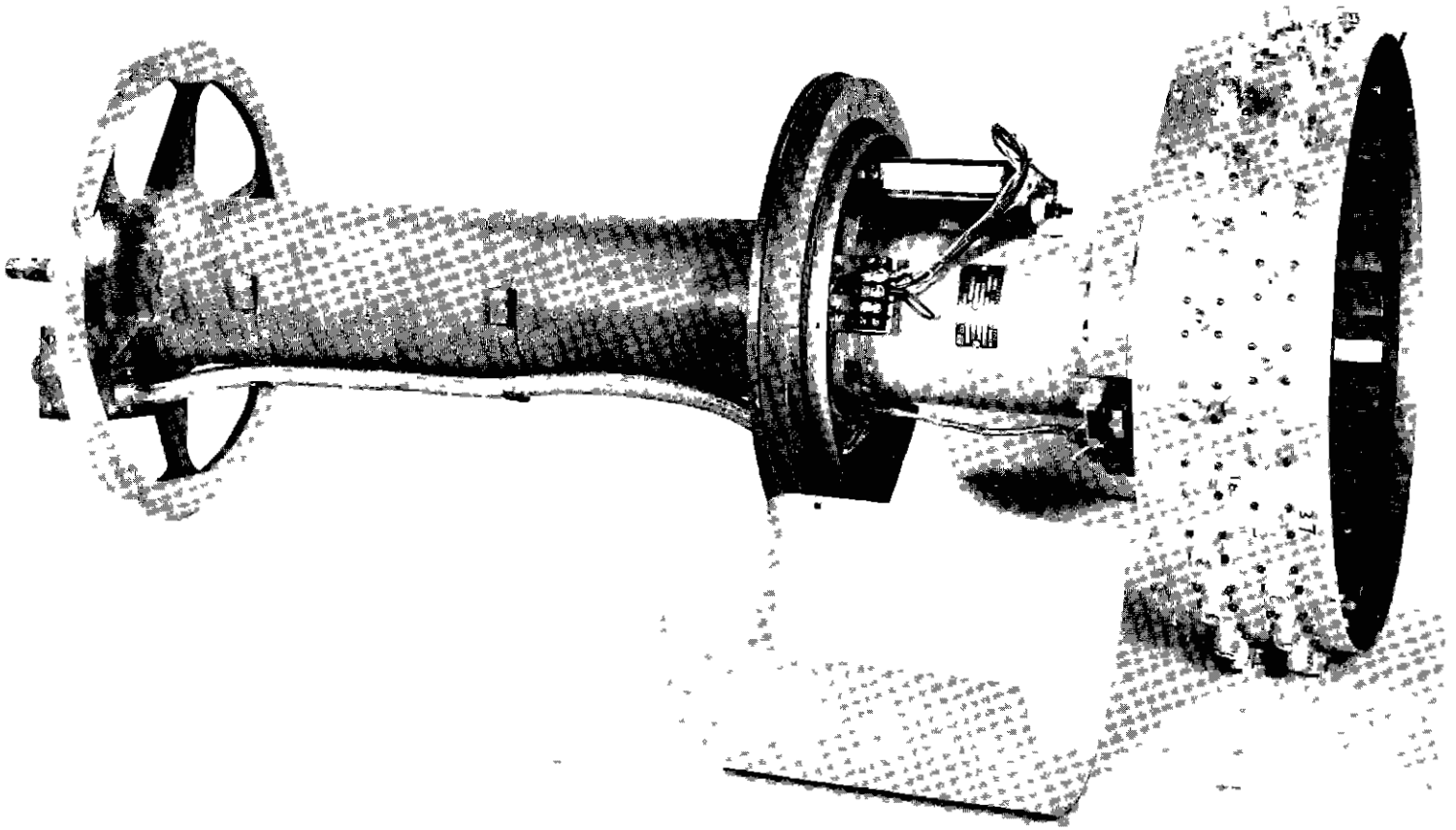

(B) DISTRIBUTOR UNIT

FIG 10 THE DOPPLER VOR DIFFERENTIAL CAPACITOR DISTRIBUTOR

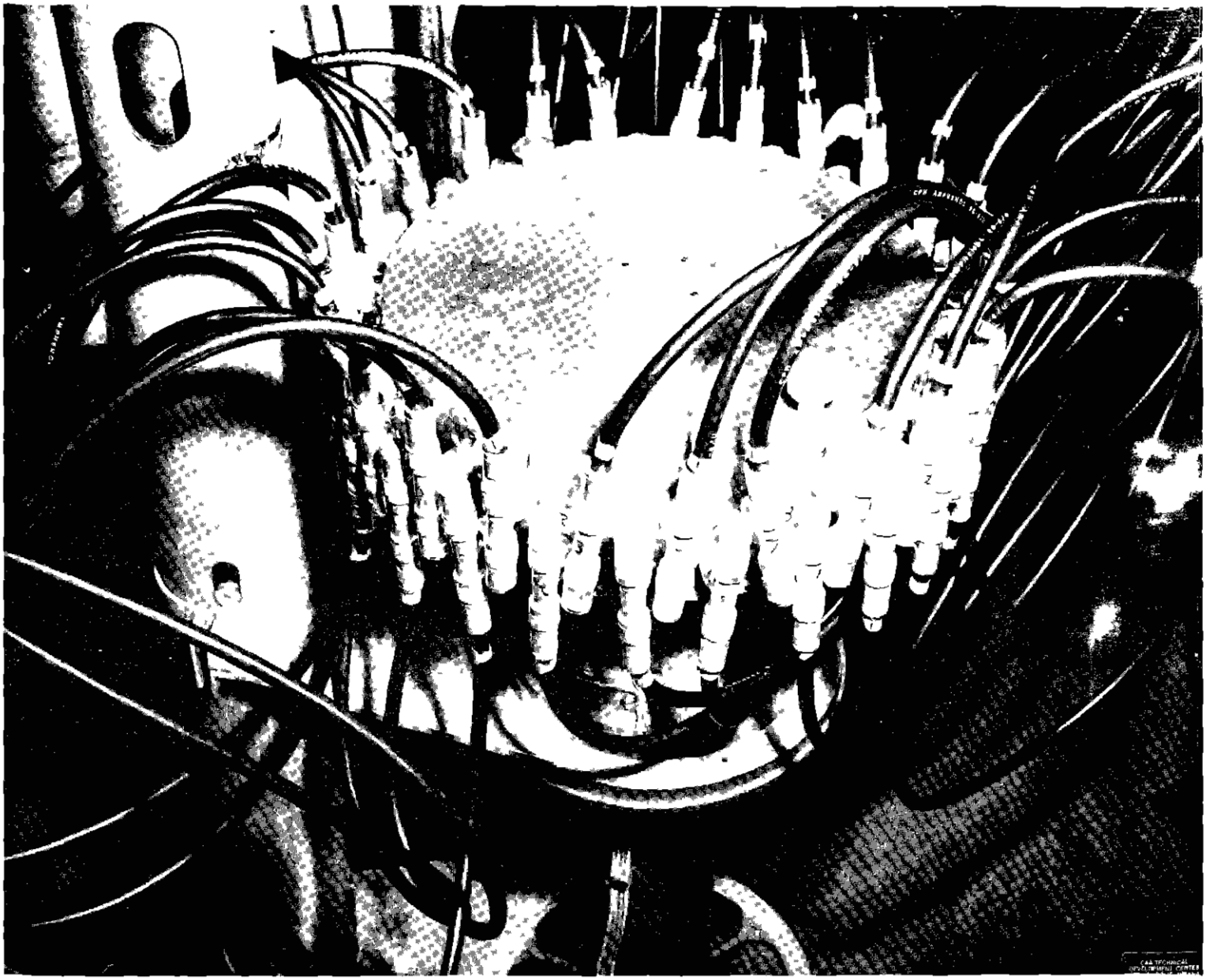

FIG. 11 DISTRIBUTOR UNIT WITH ALL LINES CONNECTED AS IN NORMAL OPERATION

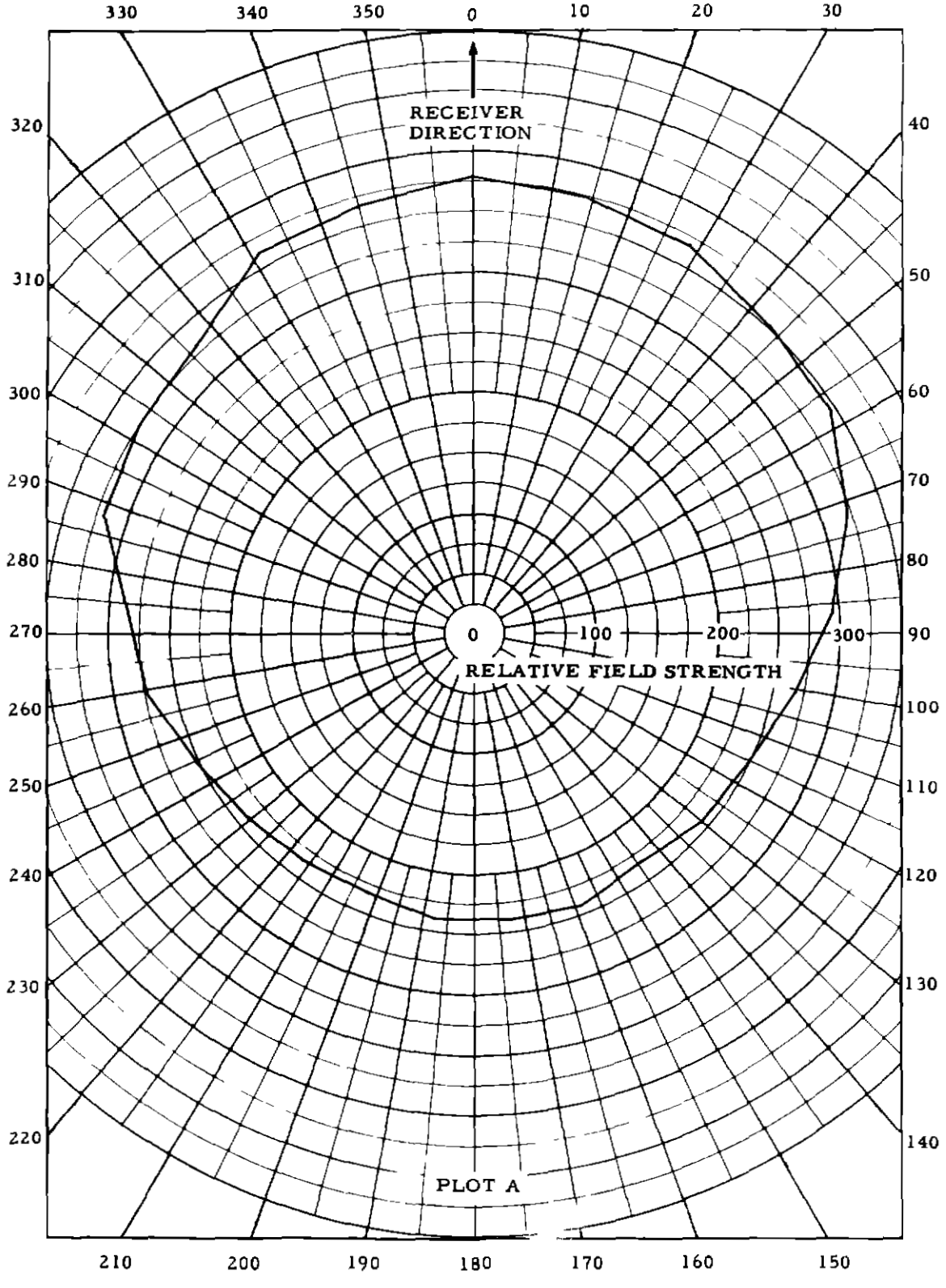

FIG 12A VARIATION IN FIELD STRENGTH OF ONE ANTENNA CAUSED BY ECCENTRICITY EFFECT OF 75-FOOT-DIAMETER COUNTERPOISE

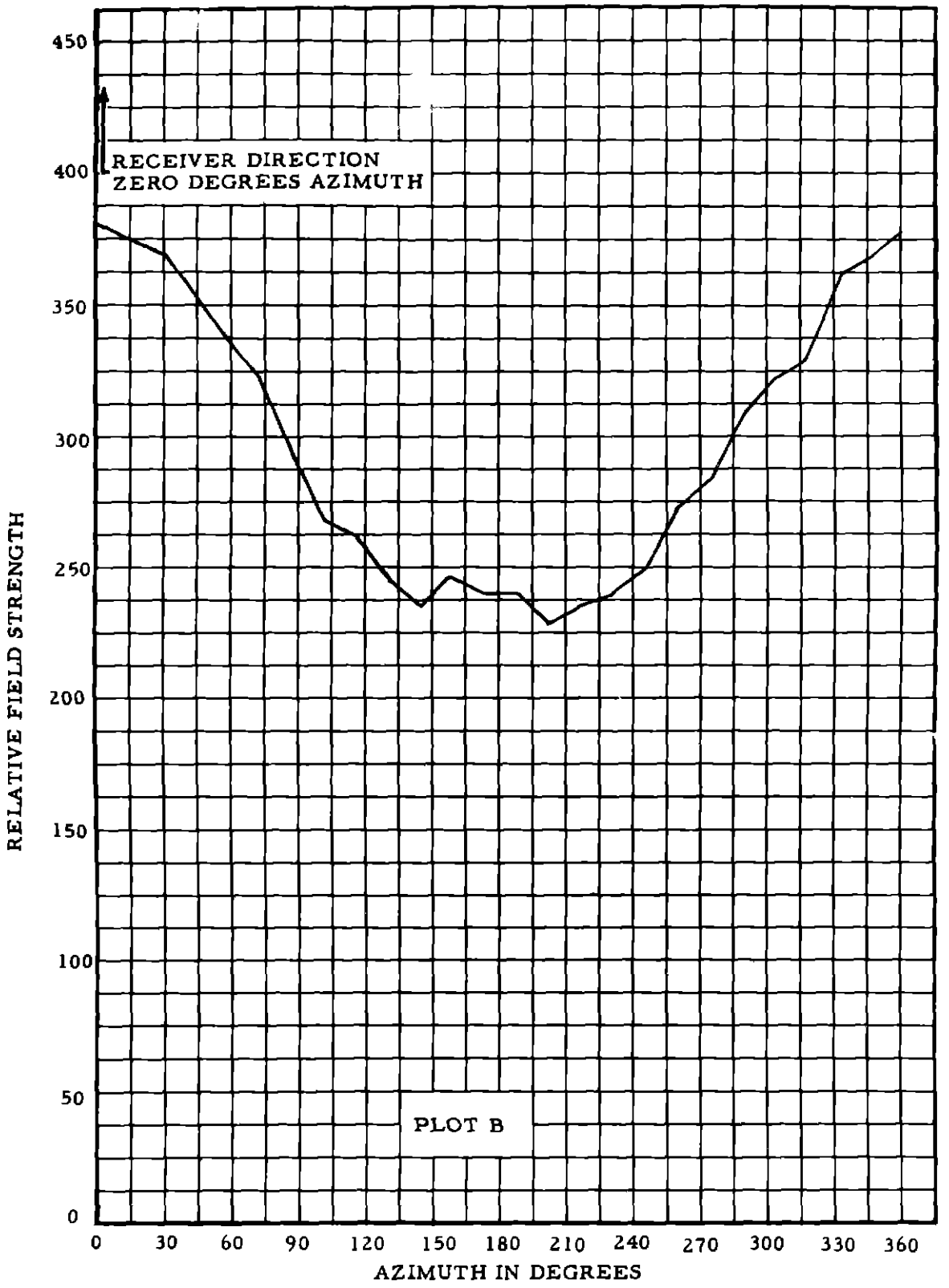

FIG. 12B VARIATION IN FIELD STRENGTH OF ONE ANTENNA CAUSED BY ECCENTRICITY EFFECT OF 75-FOOT-DIAMETER COUNTERPOISE

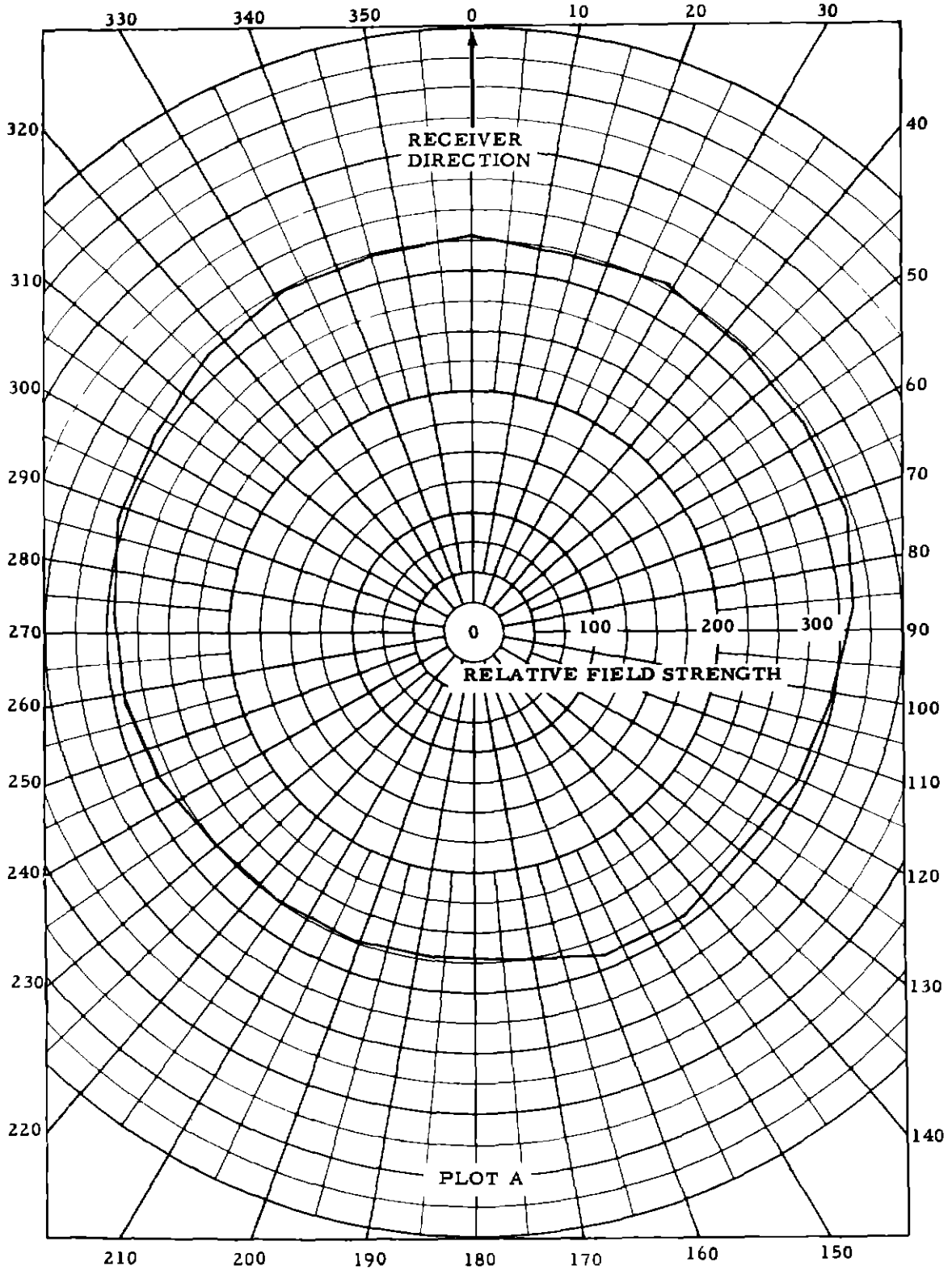

FIG 13A VARIATION IN FIELD STRENGTH C ONE ANTENNA C AUSED BY ECCENTRICITY EFFECT OF 150-FOOT-DIAMETER COUNTERPOISE

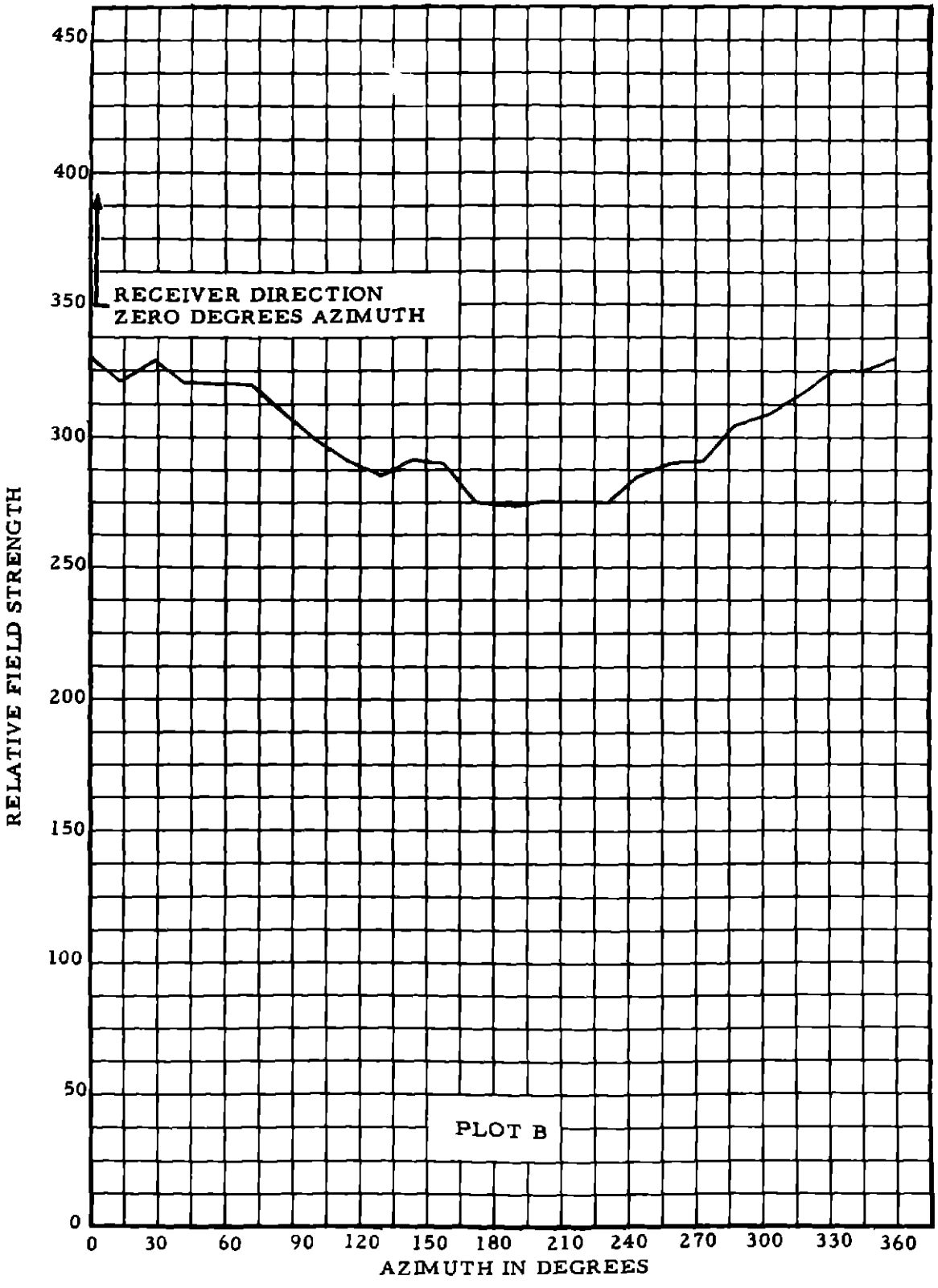

FIG 13B VARIATION IN FIELD STRENGTH OF ONE ANTENNA CAUSED BY ECCENTRICITY EFFECT OF 150-FOOT-DIAMETER COUNTERPOISE

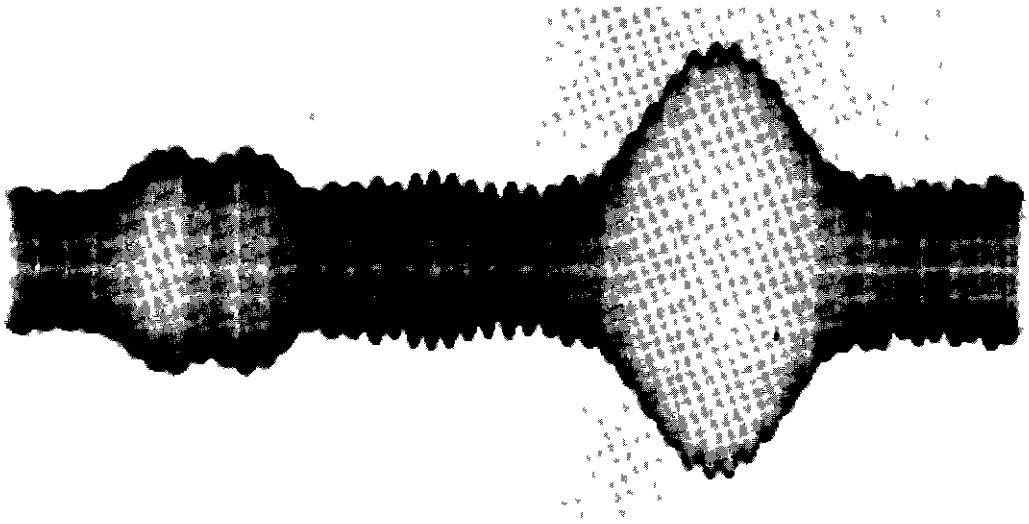

FIG. 14 PHOTO OSCILLOGRAPH OF 9960-CPS SIGNAL IN RECEIVER 200 FEET FROM STATION

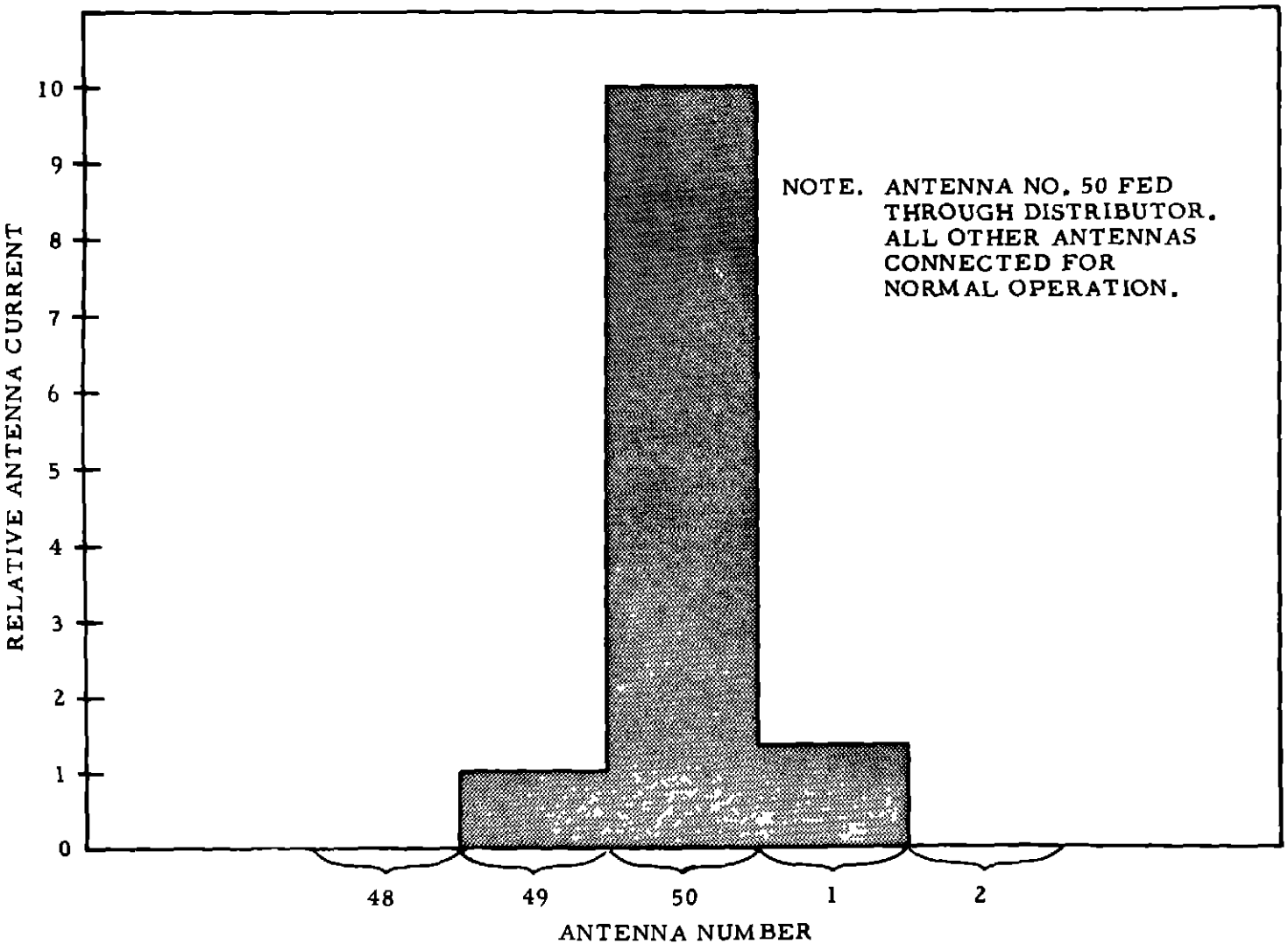

FIG. 15 ANTENNA CURRENT DISTRIBUTION WITH DISTRIBUTOR ROTOR POSITIONED TO FEED A SINGLE ANTENNA

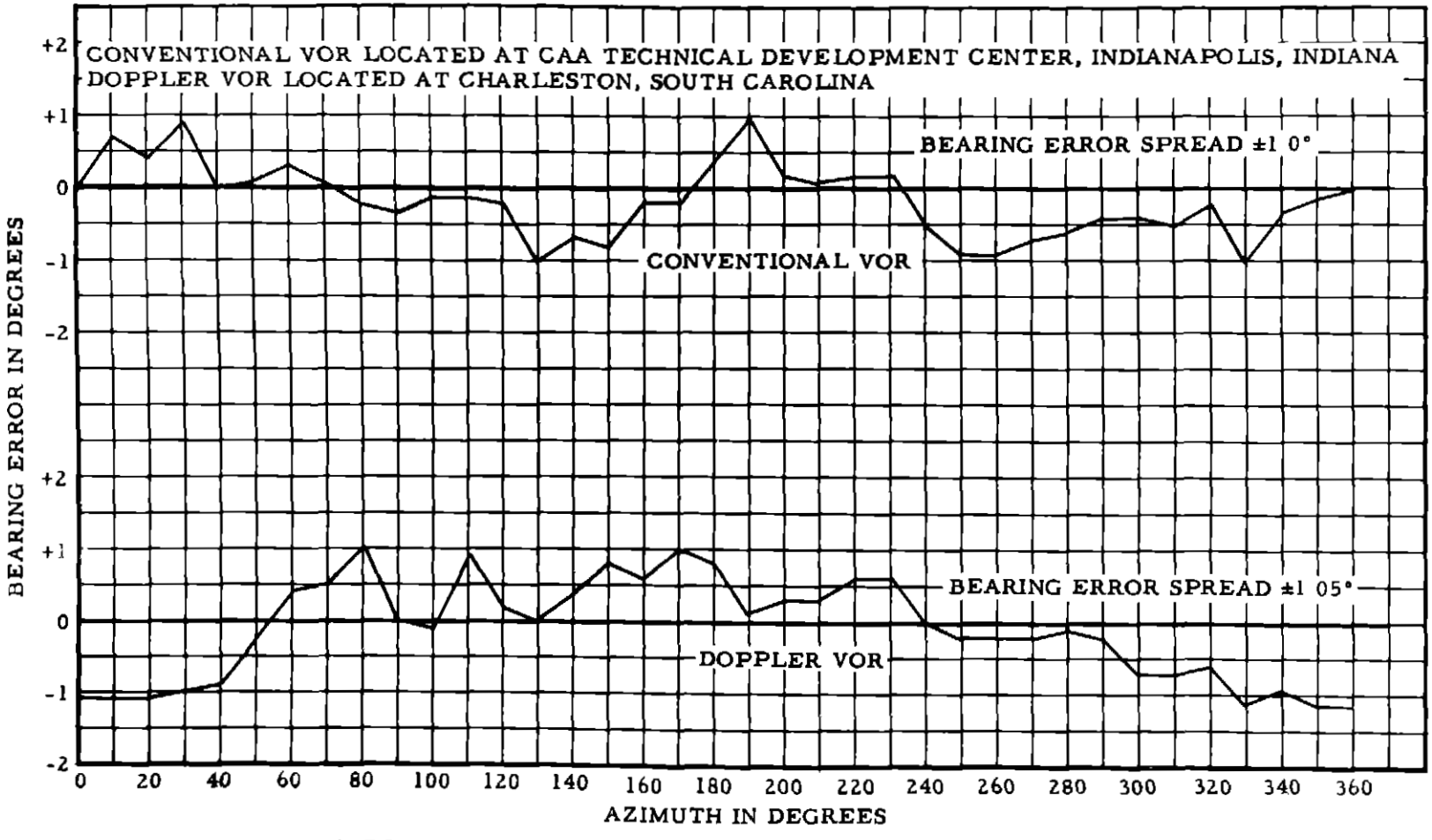

FIG 16 DOPPLER VOR AND CONVENTIONAL VOR BEARING ERROR CURVES

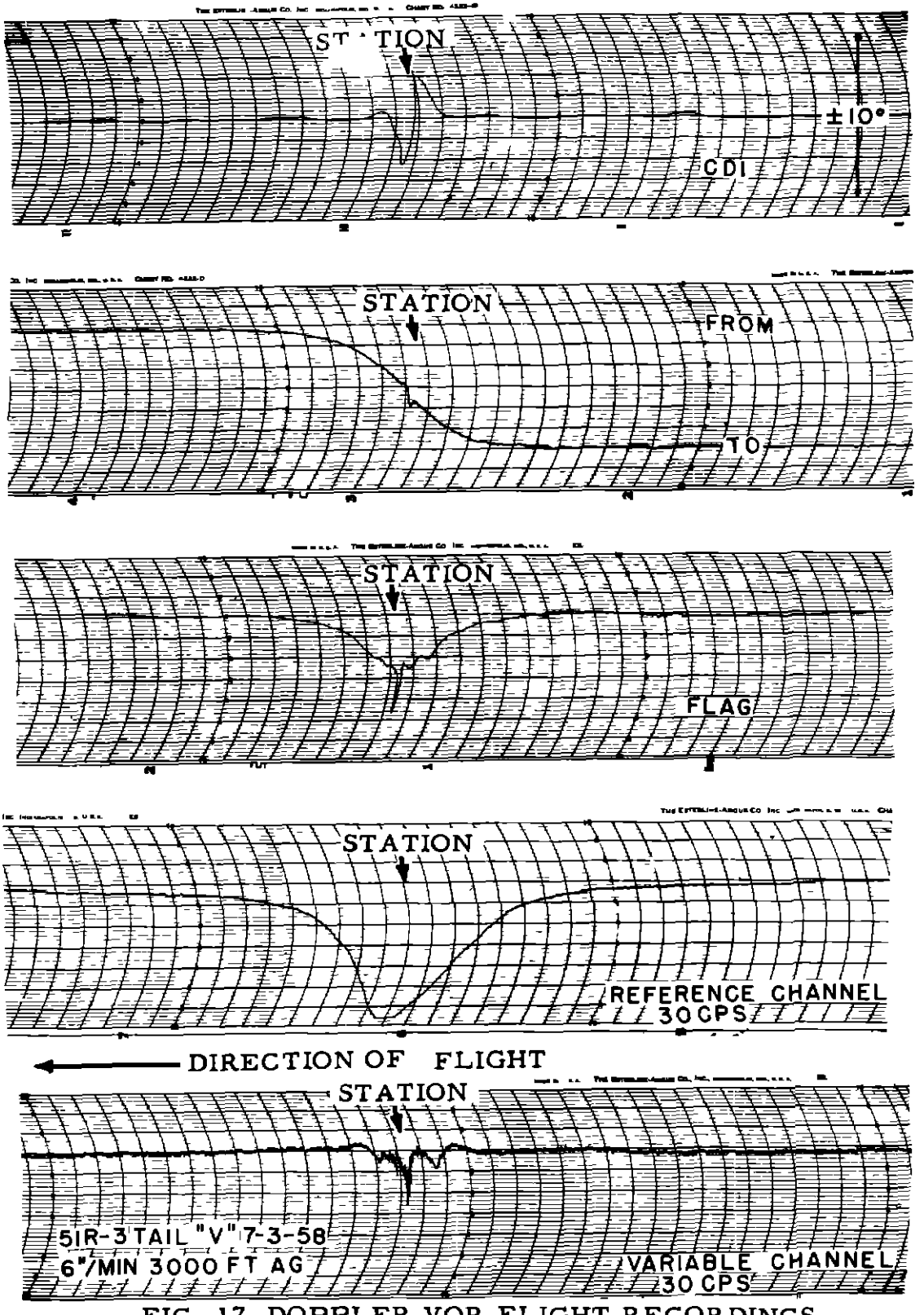

FIG. 17 DOPPLER VOR FLIGHT RECORDINGS

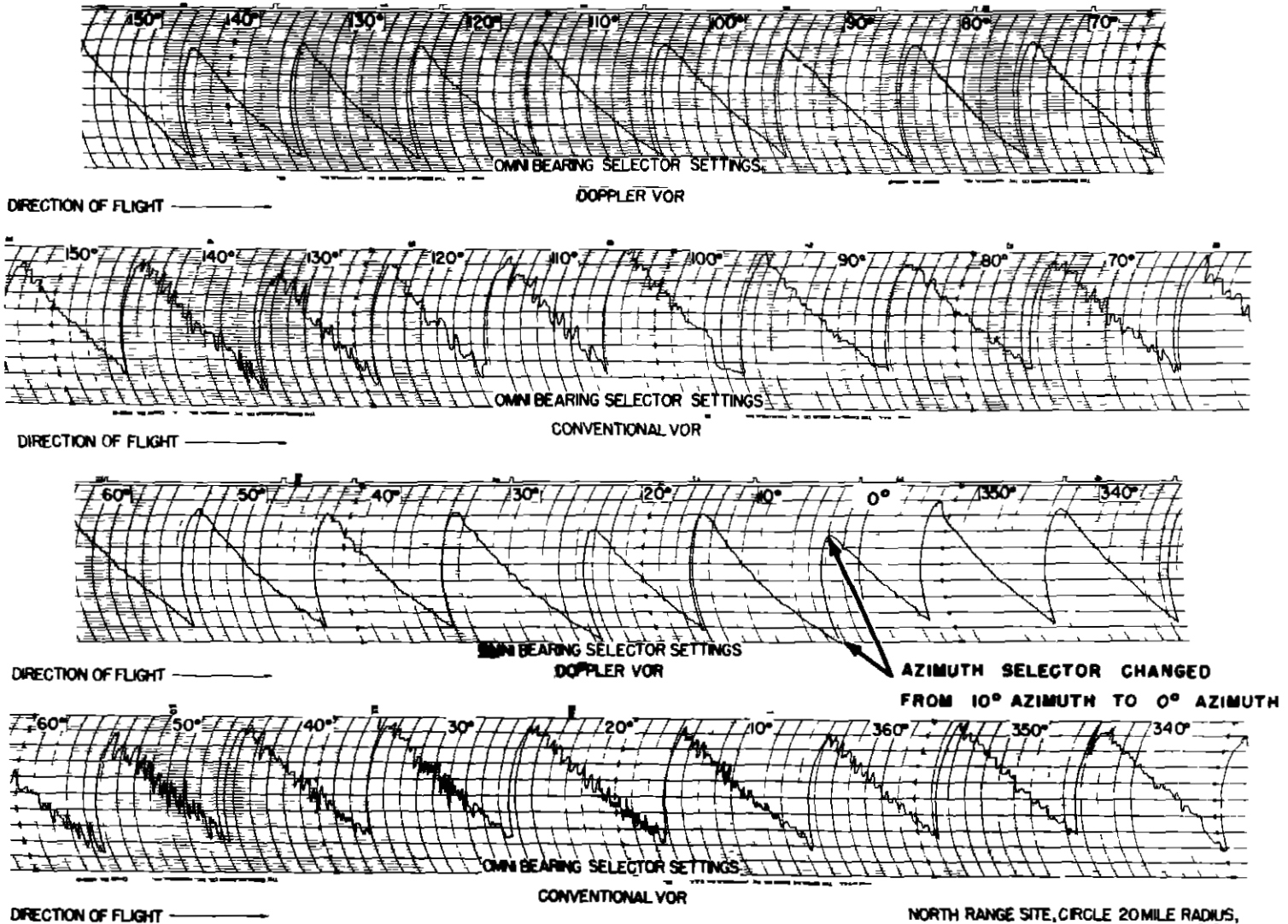

NORTH RANGE SITE, CIRCLE 20 MILE RADIUS, AIRCRAFT 1000 FT ABOVE GROUND, TAIL "V" ANTENNA, COLLINS TYPE 51[illegible]-3, N181.

PROJ NO 58-4007

FIG 18 ORBITAL FLIGHT RECORDINGS OF THE DOPPLER VOR AND THE CONVENTIONAL VOR AT THE TECHNICAL DEVELOPMENT CENTER

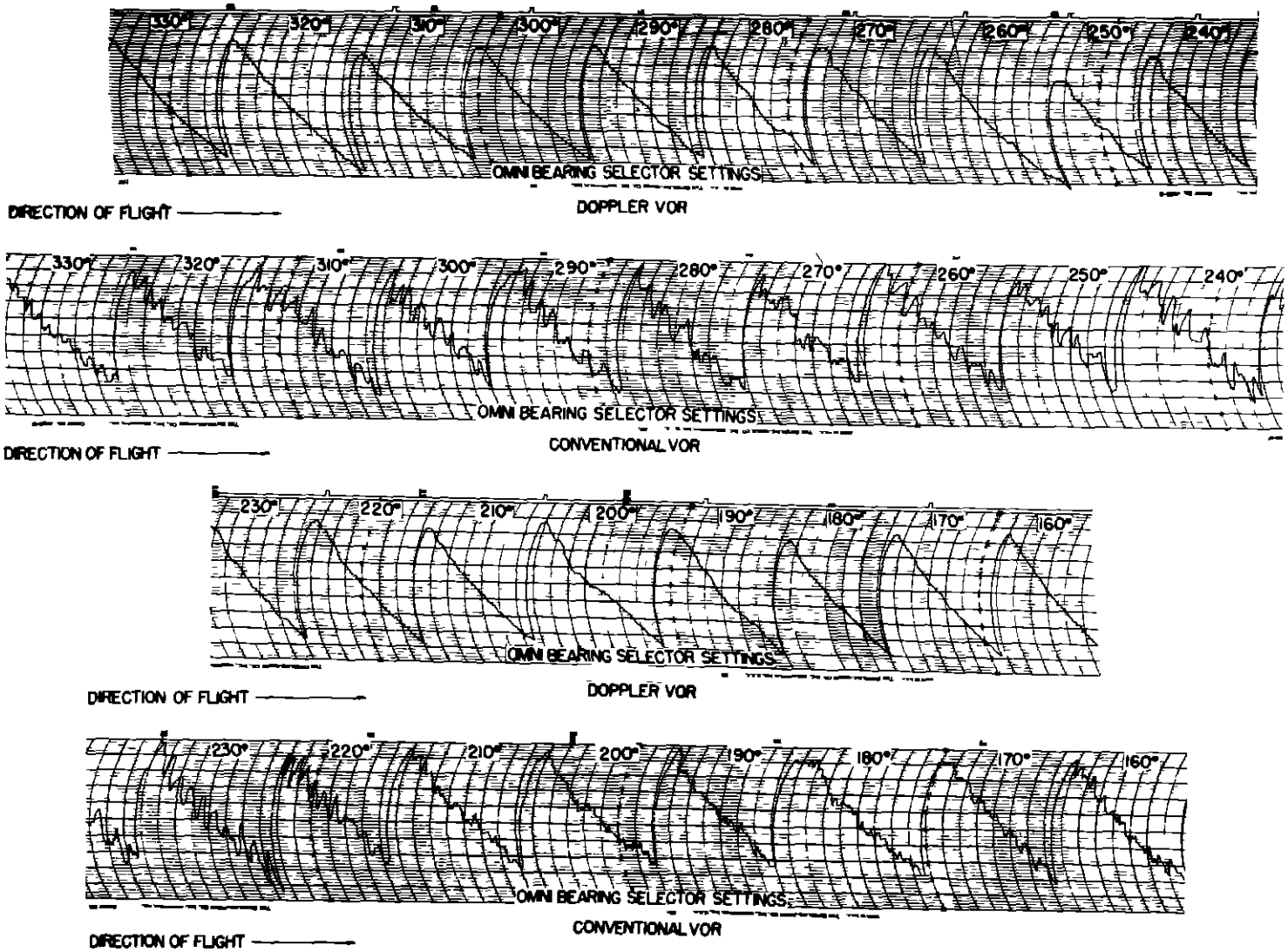

PROJ NO 58-4007

FIG 18 CONTINUED

ORBITAL FLIGHT RECORDINGS OF THE DOPPLER VOR AND THE CONVENTIONAL VOR AT THE TECHNICAL DEVELOPMENT CENTER

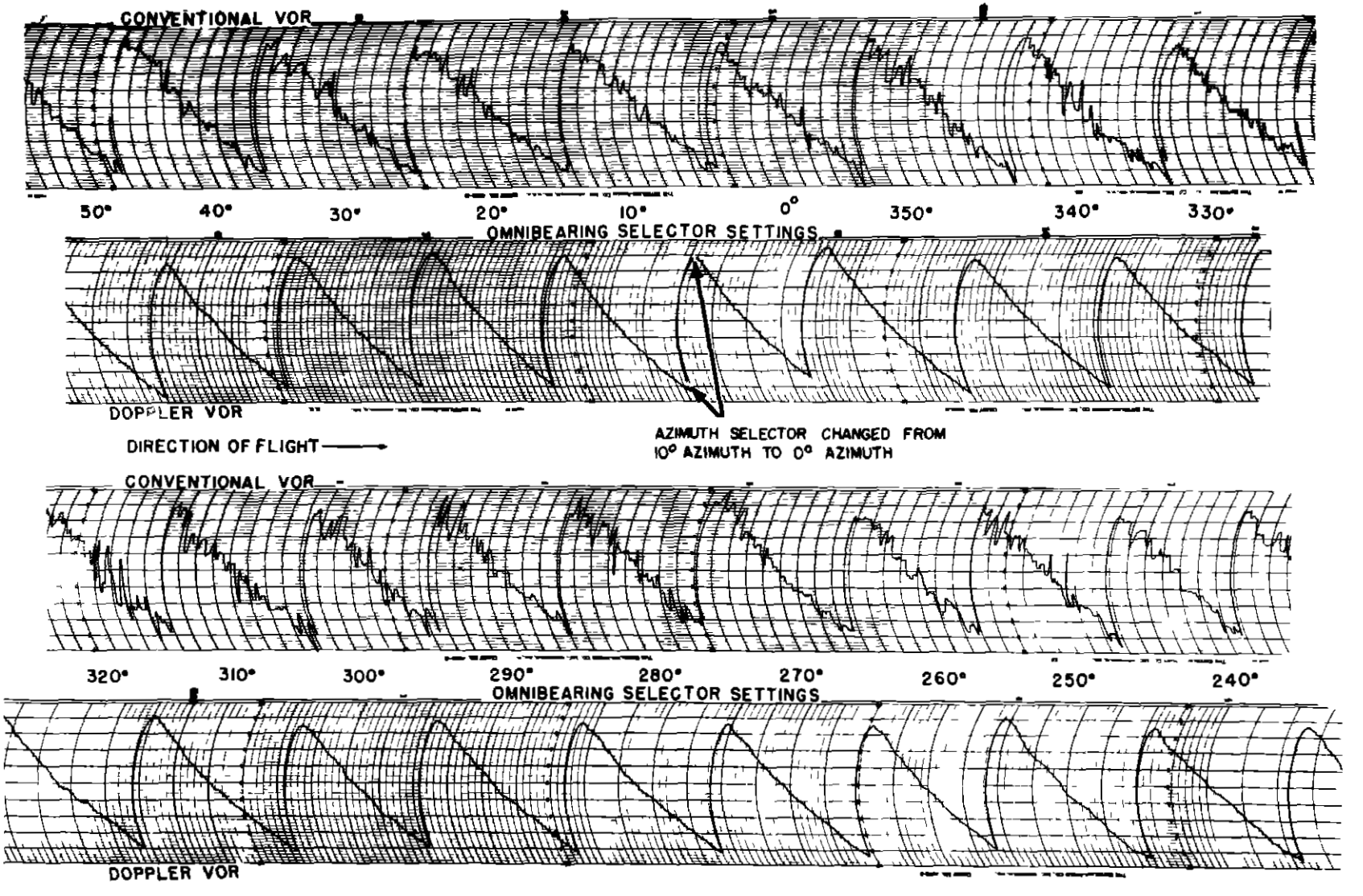

FIG 19 ORBITAL FLIGHT RECORDINGS OF THE DOPPLER VOR AND THE CONVENTIONAL VOR AT CHARLESTON, S C

CIRCLE - 20 MILE RADIUS
COLLINS 51R-3 RECEIVER
TAIL "V" ANTENNA, DC3-N182
1500 FT MSL, AUG 14, 1958

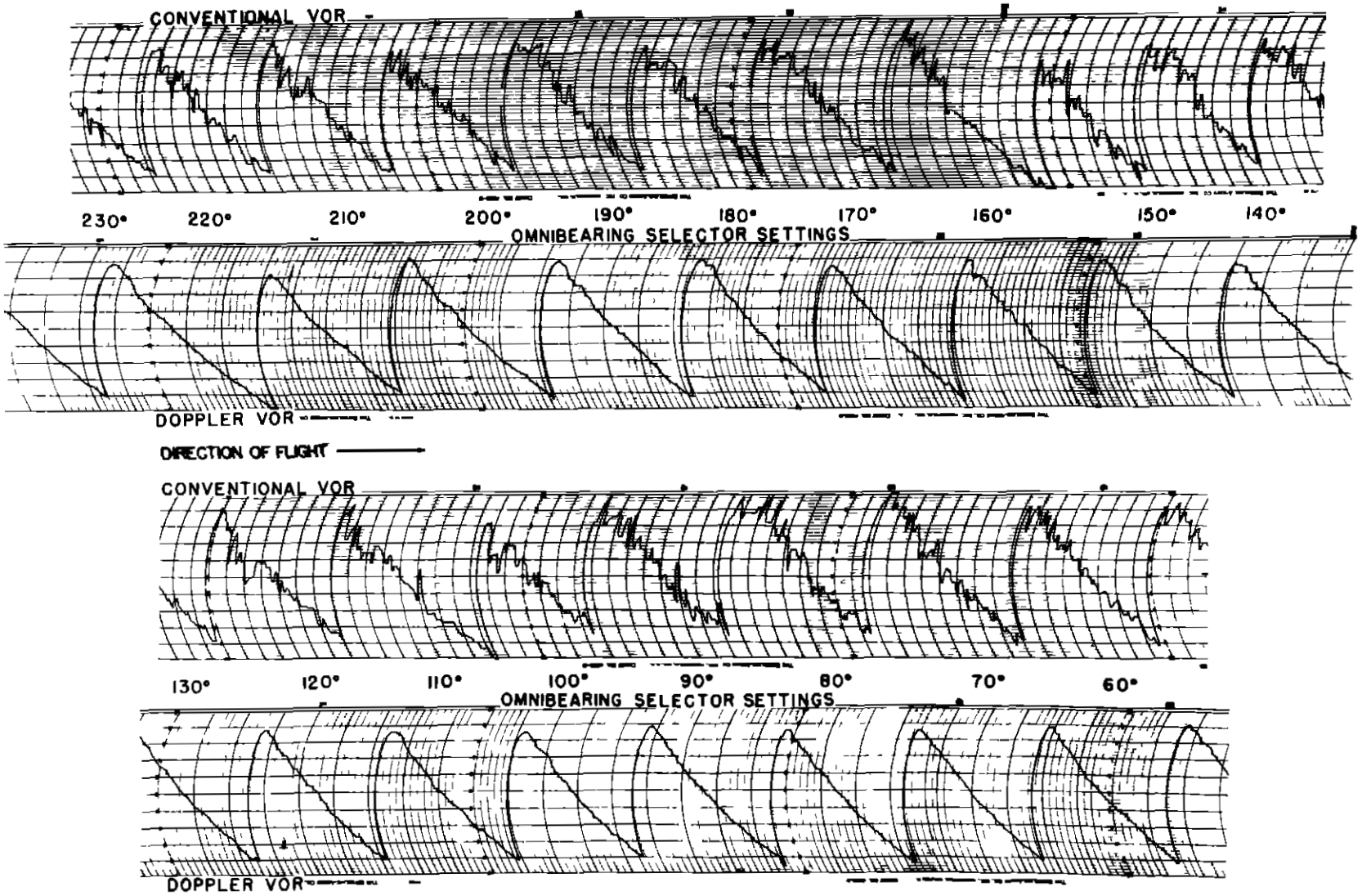

FIG 19 CONTINUED—ORBITAL FLIGHT RECORDINGS OF THE DOPPLER VOR AND THE CONVENTIONAL VOR AT CHARLESTON, S C